

Article

Targeted Luminescent Europium Peptide Conjugates: Comparative Analysis Using Maleimide and para-Nitropyridyl Linkages for Organelle Staining

David Parker, matthieu starck, Jack Fradgley, Robert Pal, Jackie Mosely, and Stefania Di Vita

Bioconjugate Chem., **Just Accepted Manuscript** • DOI: 10.1021/acs.bioconjchem.9b00735 • Publication Date (Web): 21 Nov 2019

Downloaded from pubs.acs.org on November 25, 2019

Just Accepted

“Just Accepted” manuscripts have been peer-reviewed and accepted for publication. They are posted online prior to technical editing, formatting for publication and author proofing. The American Chemical Society provides “Just Accepted” as a service to the research community to expedite the dissemination of scientific material as soon as possible after acceptance. “Just Accepted” manuscripts appear in full in PDF format accompanied by an HTML abstract. “Just Accepted” manuscripts have been fully peer reviewed, but should not be considered the official version of record. They are citable by the Digital Object Identifier (DOI®). “Just Accepted” is an optional service offered to authors. Therefore, the “Just Accepted” Web site may not include all articles that will be published in the journal. After a manuscript is technically edited and formatted, it will be removed from the “Just Accepted” Web site and published as an ASAP article. Note that technical editing may introduce minor changes to the manuscript text and/or graphics which could affect content, and all legal disclaimers and ethical guidelines that apply to the journal pertain. ACS cannot be held responsible for errors or consequences arising from the use of information contained in these “Just Accepted” manuscripts.

1
2
3
4
5
6
7
8
9
10
11
12
13
14
15
16
17
18
19
20
21
22
23
24
25
26
27
28
29
30
31
32
33

Targeted Luminescent Europium Peptide Conjugates: Comparative Analysis Using Maleimide and *para*-Nitropyridyl Linkages for Organelle Staining

11
12
13
14
15
16
17
18
19
20
21
22
23
24
25
26
27
28
29
30
31
32
33
34
35
36
37
38
39
40
41
42
43
44
45
46
47
48
49
50
51
52
53
54
55
56
57
58
59
60

Matthieu Starck, Jack D Fradgley, Stefania Di Vita, Jackie A. Mosely, Robert Pal
and David Parker*

Department of Chemistry, Durham University, South Road, Durham DH1 3LE, UK
david.parker@dur.ac.uk

Abstract

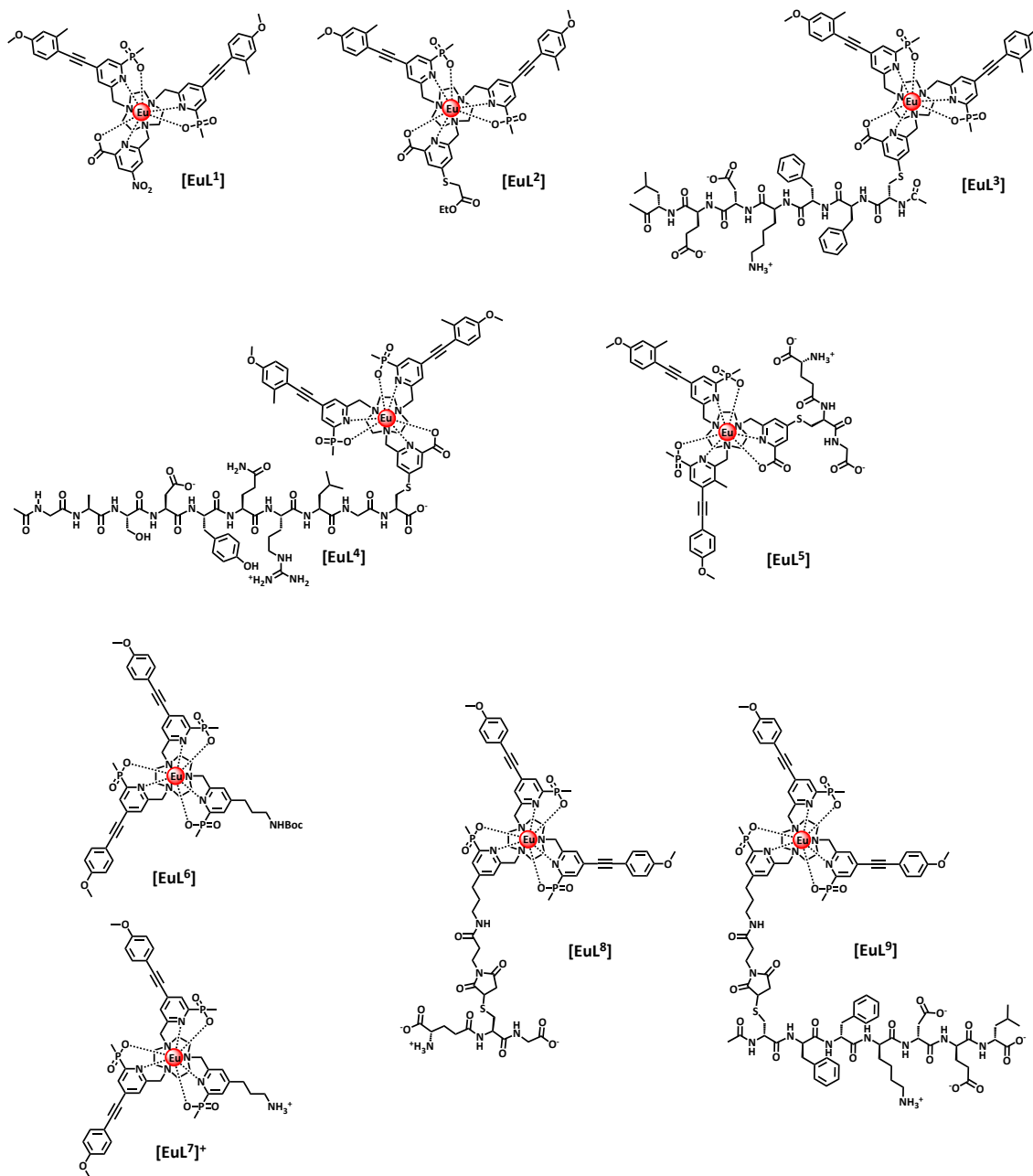
The syntheses and photophysical behaviour of nine, strongly luminescent nonadentate Eu(III) complexes are reported. Each complex is based on *N*-functionalised 1,4,7-triazacyclononane, and linkage to other groups or targeting vectors can occur either via amide bond formation to a coordinated pyridine *p*-aminopropyl group or via a nucleophilic substitution reaction involving thiol attack on a metal coordinated *p*-nitropyridyl moiety. Evidence is presented in favour of the latter conjugation strategy, as parallel work with maleimide conjugates was complicated or compromised by the propensity to undergo post-conjugation thiol exchange or succinimide ring hydrolysis reactions. Confocal microscopy and spectral imaging studies revealed that the peptide conjugate of AcCFFKDEL was found to localise selectively in the endoplasmic reticulum of mouse fibroblast cells, whereas the related maleimide conjugate was only observed in cellular lysosomes.

Introduction

Europium complexes and their bio-conjugates have been studied in depth because of their ability to serve as alternative optical stains in cell imaging or as luminescent reporters and responsive probes in a wide range of bioassays.¹⁻⁸ Early work directed towards the creation of systems that are capable of targeting a particular cell organelle assessed the intracellular uptake and localisation behaviour of scores of complexes, wherein complex charge and the nature of the sensitising aromatic chromophore were shown to have a major impact in determining the localisation profile.⁹⁻¹¹ Systems capable of selectively staining the mitochondria, (often aided by a complementary cationic complex charge) the endoplasmic reticulum, (ER), the ribosomes/nucleolus or lysosomes were identified. The common and predominant cell uptake mechanism was identified as macropinocytosis, in which the internalised macropinosome is relatively leaky and is able to discharge its contents within the cell readily.^{12,13}

Other targeting strategies can be employed in an effort to stain a particular organelle. Examples include the conjugation of a cell-penetrating peptide moiety^{14,15}, although many of these systems that use poly-cationic peptides have been shown to lead to deleterious cell toxicity, as the peptide inserts into the lipid bilayer and the cell membrane may then be permeabilised rather dramatically.¹⁶ In parallel work using fluorescent organic dyes, many reports have examined the behaviour of small peptide bio-conjugates for live cell imaging, and conjugates with BODIPY dyes that target the ER, the trans-Golgi network (TGN) and the cell nucleus have been described.¹⁷⁻¹⁹ For example, in the targeting of the ER or the TGN, peptides that carry the retention sequences KDEL and SDYQRL respectively were examined,²⁰ allowing live cell imaging of changes in morphology, dynamics and degradation.

Here, we report the synthesis and characterisation of a series of Eu(III) complexes, based on the recently described 'EuroTracker' dyes,^{21,22} in which the rare earth complex is linked to the targeting peptide vector in two different ways, (Chart 1). The first linkage method involves use of a precursor complex, [EuL¹], wherein the *para*-nitro group on a coordinated pyridine ring may be selectively displaced by a cysteine thiol group, under ambient conditions.²³ This type of linkage creates a very short tether between the metal complex and the peptide moiety, and has been used recently to prepare some Gd(III)-protein conjugates for EPR spin-labelling applications.²⁴ The second and more traditional conjugation method involves use of a maleimide moiety attached to a pendant primary amino-propyl group, as in [EuL⁷], replacing the *p*-NO₂ group in [EuL¹]. For purposes of comparison, the conjugates of glutathione, [EuL⁵] and [EuL⁸] were also prepared in this study, to assess the effect of the conjugation of this ubiquitous peptide itself, and to allow a comparison of the cell localisation profile of [EuL¹] in particular, as the nitro group could react with the endogenous glutathione *in cellulo*, during the course of observing its own localisation behaviour.

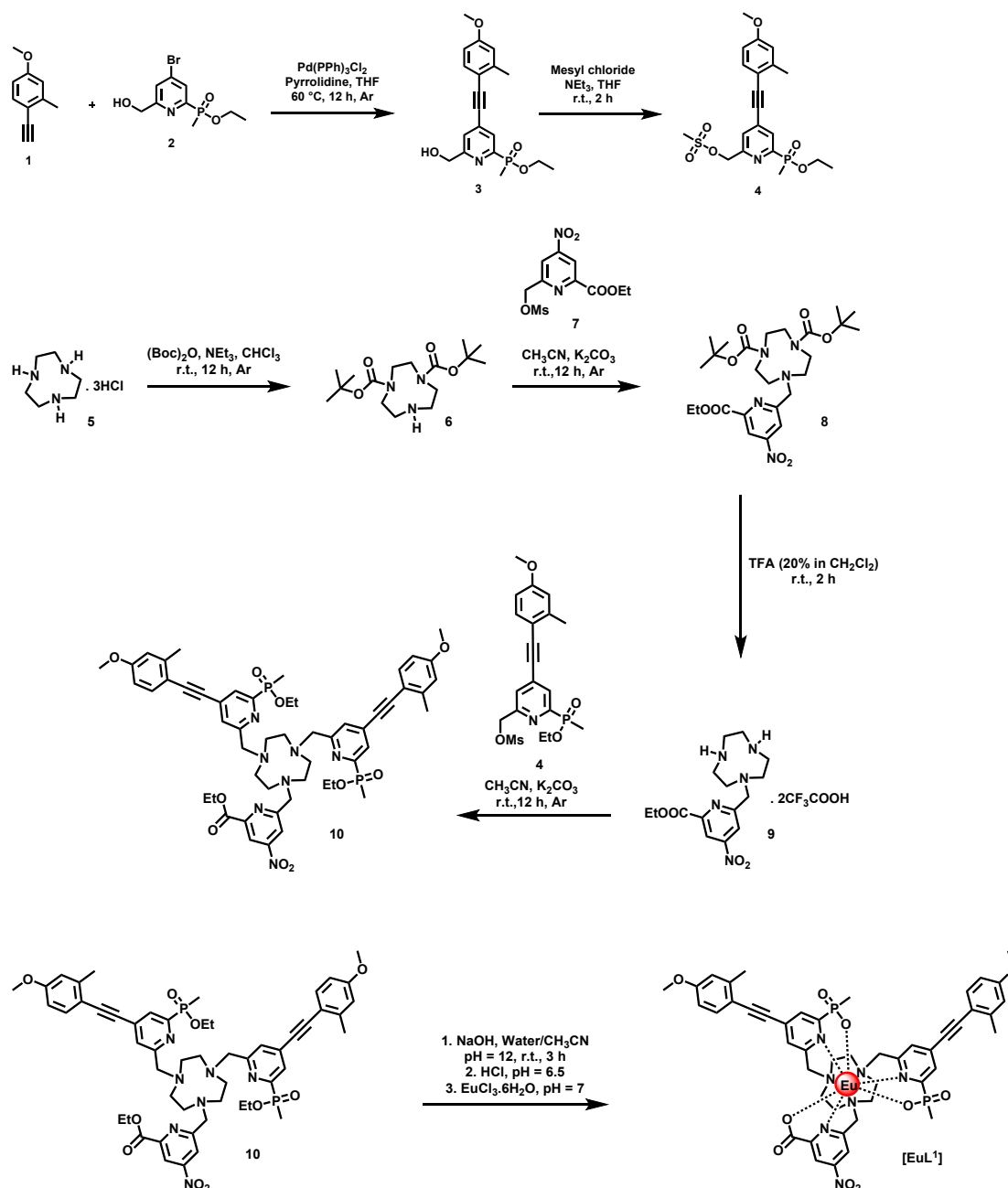


44 **Chart 1** Europium(III) complexes and selected Cys linked peptide conjugates, showing the
 45 glutathione conjugates, [EuL⁵] and [EuL⁸], the conjugates of the ER-targeting vector AcFFKDEL,
 46 [EuL³] and [EuL⁹], and the conjugate with the TGN targeting sequence, AcGASDYQLGC, [EuL⁴].
 47

48 Results and Discussion

49
 50 **Synthesis of Complexes** The syntheses of the ligands L¹ and L⁷ and their key precursors
 51 were undertaken using methods established in the recent literature.^{21,22,24} Thus, the
 52 conjugated mesylate, **4**, was prepared by the coupling reaction of **2**²¹ with the alkyne **1**
 53 mediated by catalytic Pd(PPh₃)₂Cl₂ in the presence of pyrrolidine in hot THF, followed by a
 54 standard mesylation procedure, (Scheme 1). In parallel, alkylation of di-BOC-1,4,7-
 55 triazacyclononane, **6**, with the *p*-nitromesylate **7**,²⁴ followed by treatment with TFA gave the
 56
 57
 58
 59
 60

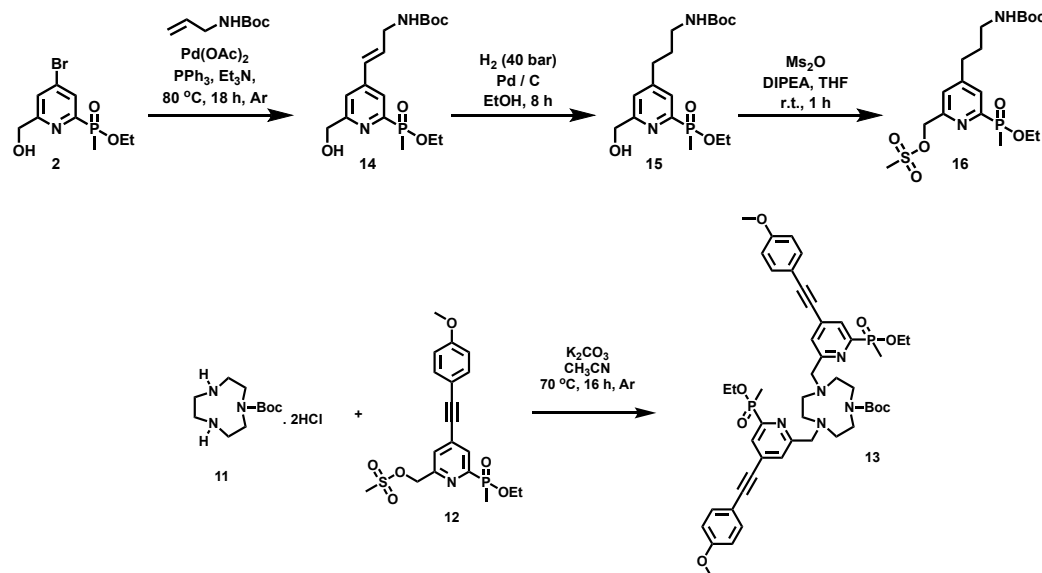
amine **9**, and the key ligand precursor **10** was obtained by reaction with two equivalents of the mesylate, **4**. Base hydrolysis followed by complexation with europium chloride at ambient pH gave the charge neutral complex [EuL¹] that was purified by reverse phase HPLC, (see SI).



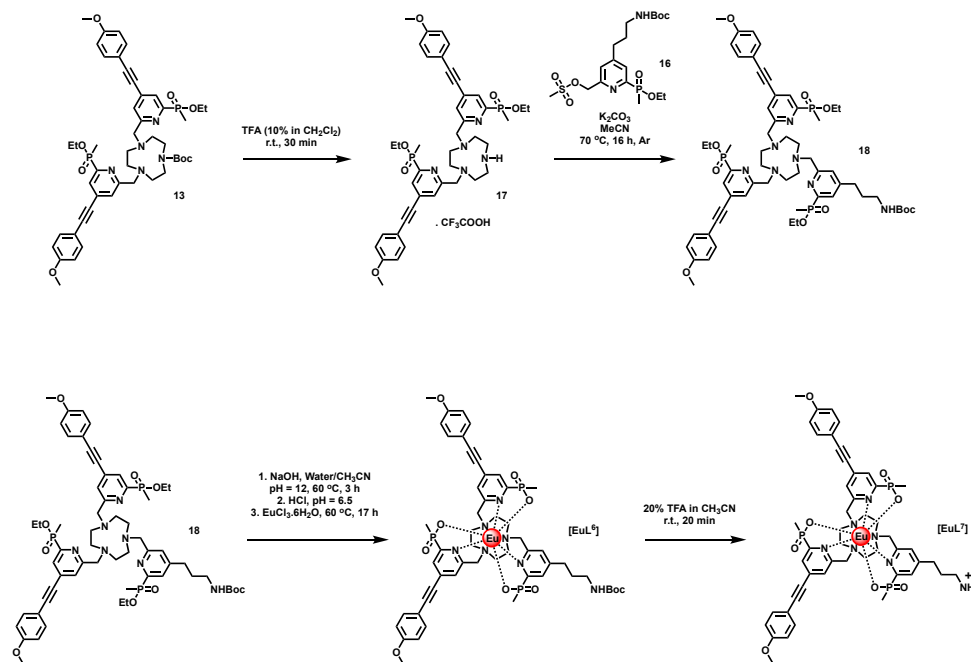
Scheme 1 Synthesis of the ligand precursor, **10**, and the derived Eu(III) complex, [EuL¹]

The complex, [EuL⁷] was prepared using similar methodology, Schemes 2, 3 and 4. In its structure, the amino-propyl group replaces the *p*-nitro group in L¹, and the primary amine allows a variety of conventional coupling methodologies to be used. Here, we converted it *in situ* into a maleimide moiety, in order to permit selective reaction with the cysteine thiol group in the peptides. Reaction of the common intermediate, **2**, with N-Boc-allylamine under Pd catalysis gave the alkene, **14**, together with its constitutional isomer, where the

double bond is not conjugated to the pyridine. Hydrogenation over palladium on carbon gave the alcohol **15** only, and mesylation using methanesulfonic anhydride afforded the ester **16**. Subsequent steps to the ligand precursor **18** were carried out by stepwise N-alkylation and standard de-protection methods, and the complex $[\text{EuL}^7]$ was finally prepared by reaction of the complex $[\text{EuL}^6]$ with TFA in MeCN for 20 minutes. Under these relatively mild conditions, the Eu complex resists acid-catalysed decomplexation.

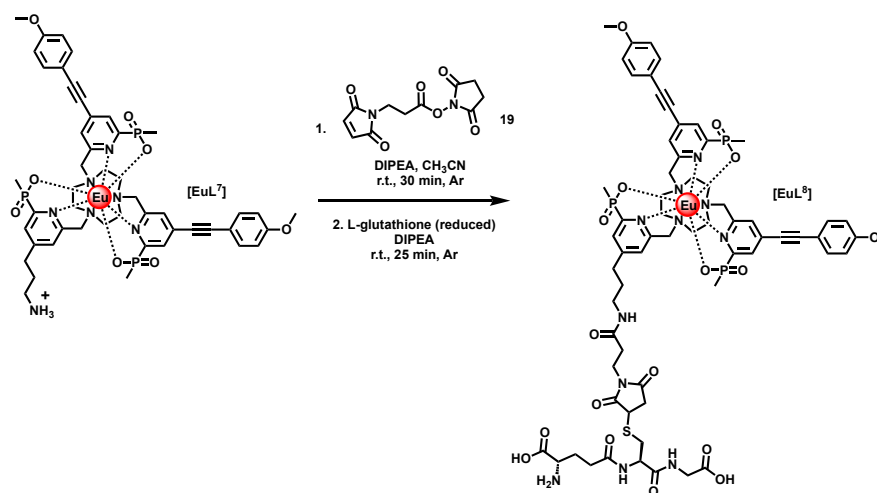


Scheme 2 Synthesis of the intermediate mesylate **16**, and the carbamate **13**



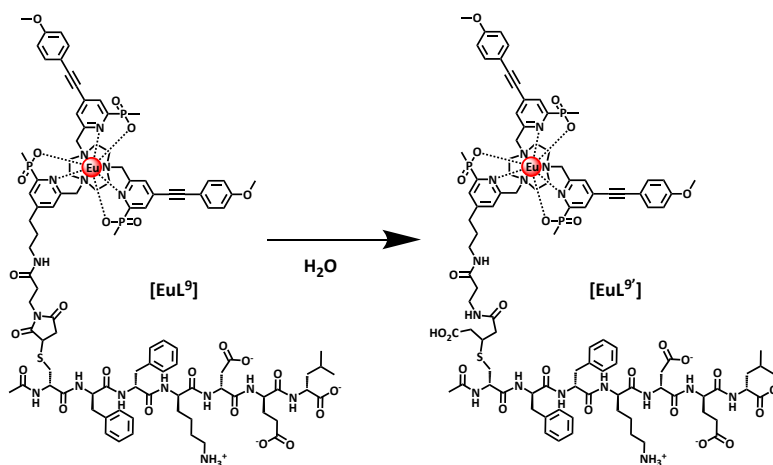
Scheme 3 Synthesis of the *p*-aminopropyl functionalised complex, $[\text{EuL}^7]$

Finally, the primary amino group was reacted with the maleimide active ester, **19**, from which the peptide conjugates were derived, e.g. the glutathione adduct, $[\text{EuL}^8]$, Scheme 4.



Scheme 4 Synthesis of the glutathione conjugate, [EuL⁸]

Proof of the constitution of the peptide adducts was obtained from a series of MS-MS fragmentation experiments, (Figures 1 and 2), aided by the presence of the characteristic Eu isotope pattern in certain fragments. Thus, the parent species of [EuL³] was observed as a doubly charged ion, [M+2H]²⁺, and the observation of successive fragmentation from the C-terminus enabled confirmation that the Cys thiol group had displaced the *p*-nitro group in [EuL¹]. This analysis was confirmed by the observation of fragments derived from cleavage around the thio-ether bond linkage site. Similar methods were used to establish the constitution of [EuL⁹]. Here, an additional species was observed, identified also by LCMS, that corresponded to the ring-opened adduct (i.e. M + 18) where the succinimide moiety reacts with water following thiol addition, (Scheme 5 and Figure 2). The ratio of the two species varied slightly in separate reactions, but was estimated by LC peak integration to be 3:2, in favour of the ring opened adduct. Such competitive hydrolysis reactions have been observed previously in maleimide conjugation chemistry,²⁵ and contrast with the clean substitution reaction using [EuL¹]. Indeed, the stability of the thiol/maleimide adduct has been a cause of concern, as subsequent thiol exchange may adversely compromise conjugate stability. The hydrolysed, ring-opened product on the other hand, shows an enhanced stability towards cleavage of the C-S bond, and is preferred.²⁵



Scheme 5 Formation of the hydrolysed adduct following thiol attack on the maleimide

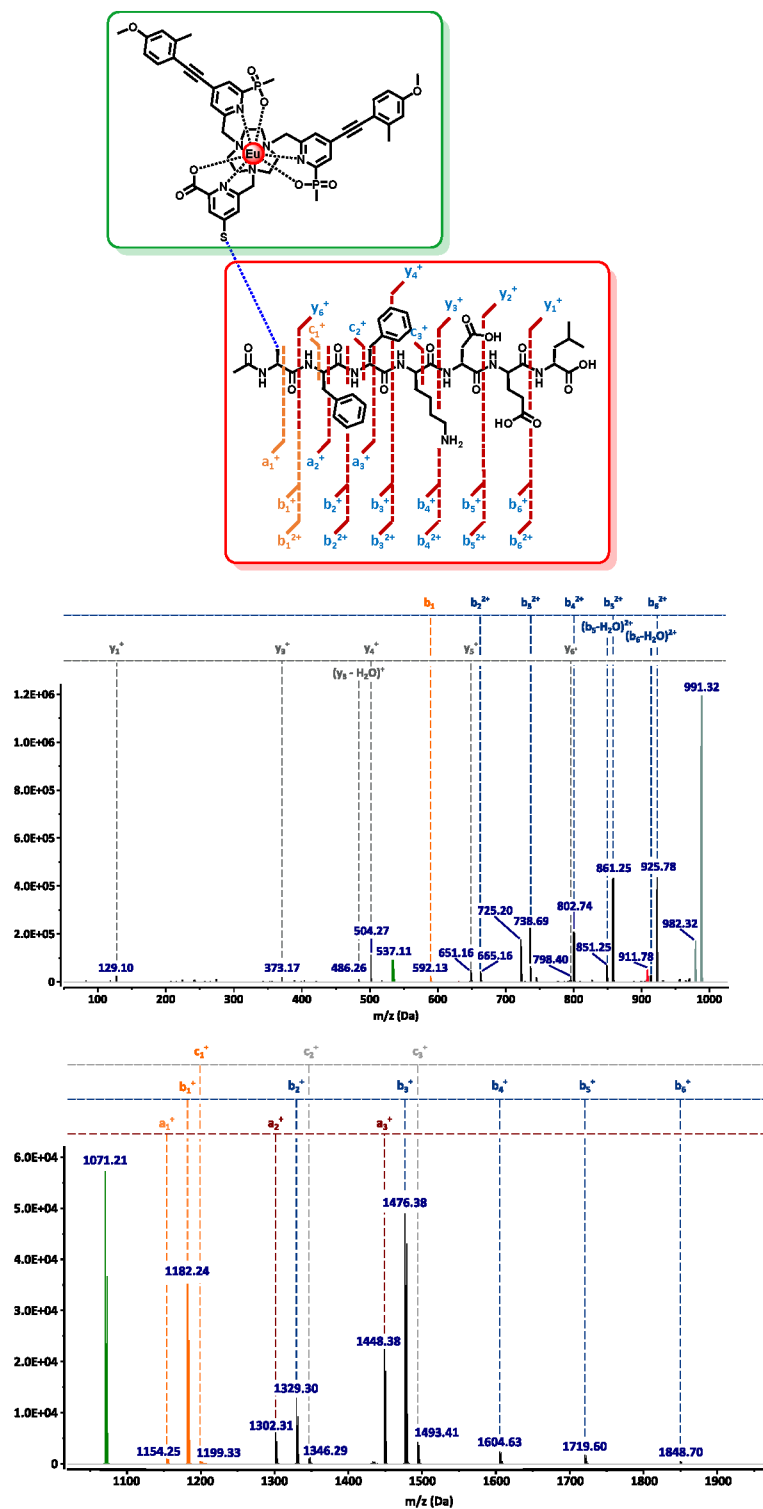


Figure 1. $[EuL^3]$ LC/MS-MS Analysis. Fragmentation patterns enabling proof of constitution of the peptide conjugate $[EuL^3]$. Peaks corresponding to the Eu labelled peptide at $m/z = 991$ Dalton $[M+2H]^{2+}$ and 982 Dalton $[M+2H-H_2O]^{2+}$. Orange peaks (a_1^+ , b_1^+ , b_1^{2+} and c_1^+) are diagnostic peaks showing that the fragment containing the cysteine side-chain is conjugated to the complex. Green peaks correspond to fragmentation close to the thio-ether bond, as represented in the upper scheme, giving the fragments $[(\text{peptide-SH})+H]^+$ ($m/z = 911$ Dalton) and $[(\text{complex SH}) + H]^+$ and $[(\text{complex SH}) + 2H]^{2+}$ ($m/z = 1071$ D and 537 D respectively).

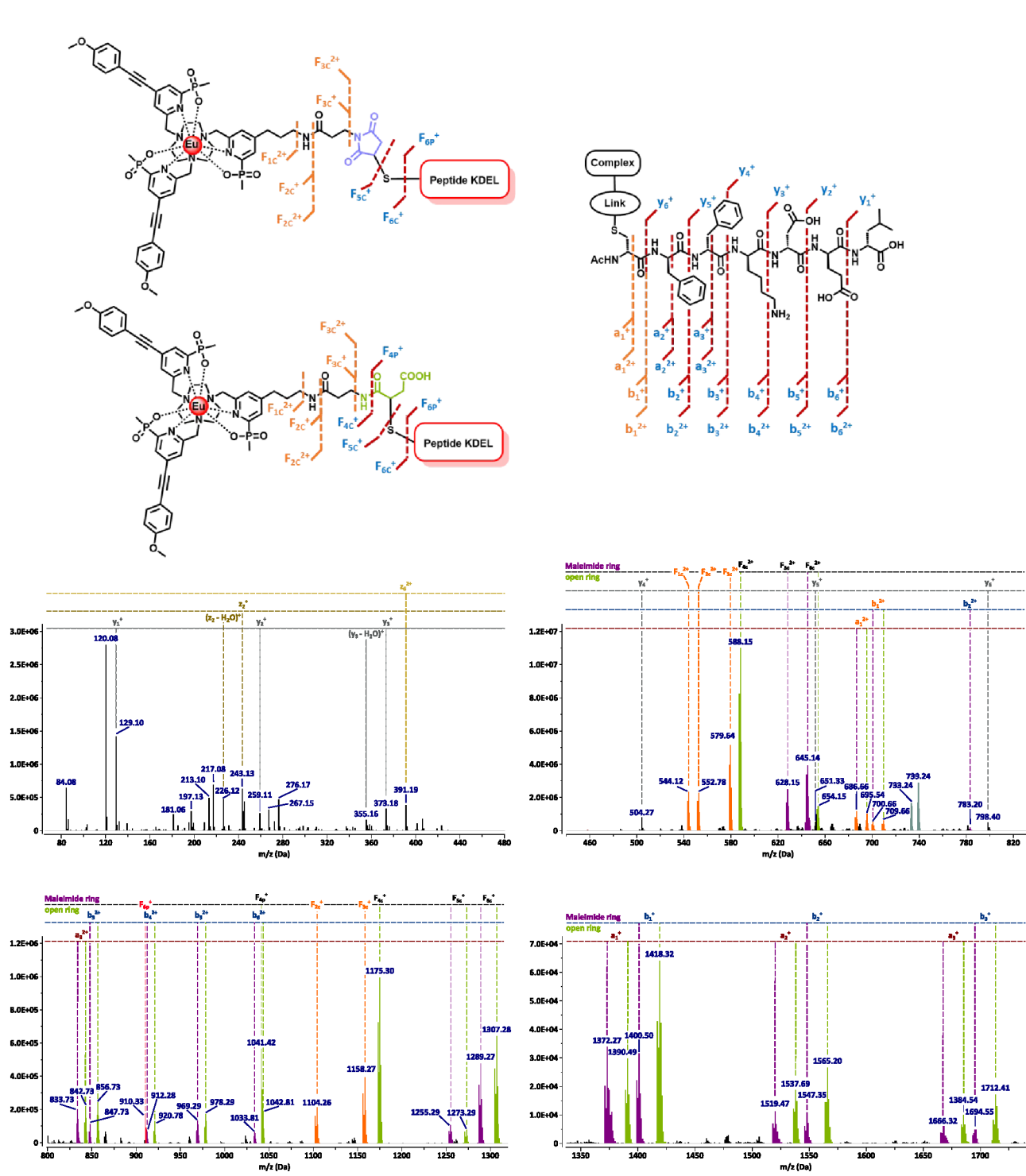


Figure 2. $[EuL^9]$ LC/MS-MS Analysis. MS-MS Fragmentation patterns enabling proof of constitution of the peptide conjugate, $[EuL^9]$. Peaks at $m/z = 733.24$ and 739.24 Dalton $[M+3H]^{3+}$ correspond to the Eu labelled peptide with maleimide derived and ring-opened maleimide derived moieties, respectively. Orange peaks (F_{1C} , F_{2C} , F_{3C} , a_1 and b_1) and the fragment F_{6P} ($[(\text{peptide-SH})+H]^+$ at $m/z = 911$ Dalton) are diagnostic peaks proving that the peptide/complex conjugation using the maleimide (cyclic or the ring-opened hydrolysed derivative) moiety occurs chemoselectively with the cysteine thiol group

In the case of [EuL⁸], the glutathione adduct was isolated as the cyclic succinimide conjugate only. In order to assess its stability to thiol exchange and hydrolytic ring opening, it was allowed to react in ammonium bicarbonate buffer with 2 equivalents of ethyl thioglycolate at 295K. The related adduct [EuL⁵] was examined in parallel and progress of each reaction monitored over 24h using LCMS. With [EuL⁸], within 2h free glutathione was detected; none was detected with [EuL⁵] even after 24h. Furthermore, adducts arising from glutathione displacement and addition with ethyl thioglycolate were observed for [EuL⁸] at 1392 and 1374D (and at half mass with characteristic Eu isotope patterns), corresponding to the hydrolysed [M + 18]⁺ and succinimidyl conjugates respectively. No such corresponding masses were observed for [EuL⁵]. In each case, beyond periods of 12h a minor species (<10%) was detected with a mass of the parent complex plus 120, corresponding to slow conjugate addition of ethylthioglycolate to the pyridyl-alkyne electrophile. Taken together, these observations support the conclusions reached by Santi et al²⁵, and affirm the chemical stability of the thiopyridine conjugate to thiol exchange that limits the utility of certain classical maleimide conjugates.

Photophysical Data for Eu(III) Complexes

Absorption, emission and excitation spectra for the Eu complex-peptide conjugates were measured at 295 K in water at pH 7.5 and in D₂O, (Table 1 and Figures 3-6). In each case, measurements of the radiative rate constants for depopulation of the Eu ⁵D₀ excited state in water and D₂O allowed the metal hydration state, *q*, to be estimated to be zero,²⁶ consistent with cooperative binding of the six ligand nitrogen atoms and the three ionised oxygen atoms. The form of the Eu emission spectral profile was more or less unchanged, comparing [EuL¹] with [EuL³] and [EuL⁴], although minor differences were observed in the hypersensitive $\Delta J = 4$ manifold around 680-710 nm for the complexes of [EuL⁸] and [EuL⁹].

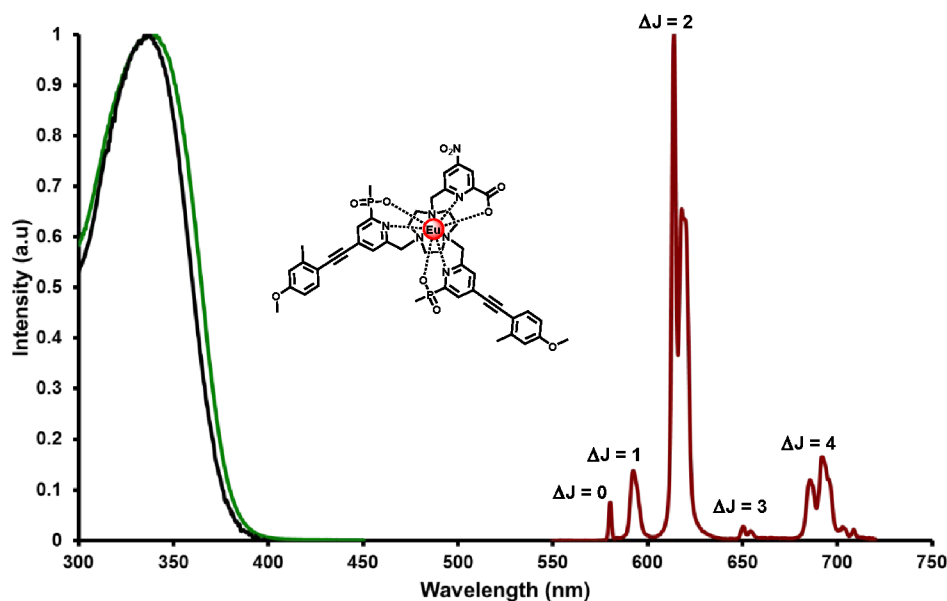
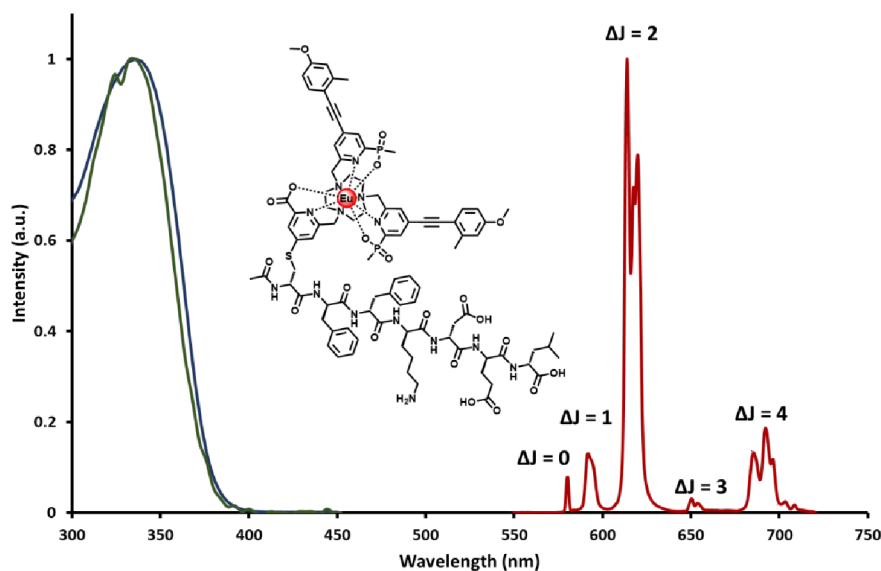


Figure 3. Photophysical spectra for [EuL¹] (30 μ M in aq. ammonium bicarbonate solution, 25 mM, pH 7.5): absorbance (green), excitation (blue, $\lambda_{em} = 614$ nm), emission (red, $\lambda_{exc} = 340$ nm).

Table 1. Summary of photophysical properties determined for Eu(III) complexes in water and D₂O^a.

Complexes	$\lambda_{\text{max}} / \text{nm}$	$\epsilon / \text{M}^{-1}\text{cm}^{-1}$	$\tau / \text{ms} \pm 10\%$	q	$\phi / \%$	$B / \text{M}^{-1}\text{cm}^{-1}$
EuL ¹	340	42000	0.87 1.05 ^a	0	5 ± 1	2120
EuL ²	340	41000	0.93	0	15 ± 2	6180
EuL ³	336	41000	0.93	0	16 ± 2	6600
EuL ⁴	336	41000	0.93	0	18 ± 3	7420
EuL ⁵	336	41000	0.93	0	20 ± 3	8200
EuL ⁶	328	31000	1.11 1.27 ^a	0	33 ± 5	10230
EuL ⁸	328	31000	1.09	0	28 ± 4	8680
EuL ⁹	328	31000	1.09	0	39 ± 6	12100

With [EuL¹] the presence of the *p*-NO₂ group in the non-conjugated pyridyl part of the complex leads to a reduced overall emission quantum yield, presumably due to competitive photo-induced electron transfer from the extended chromophore excited state to the local LUMO in this moiety. The overall emission quantum yields for the peptide conjugates were quite high, notably for the conjugates with a trimethylphosphinate europium coordination environment, that provides increased conformational rigidity and gives rise to more effective steric shielding of the Eu(III) excited state from vibrational energy transfer quenching.²¹

**Figure 4.** Photophysical spectra for [EuL³] (9.4 μM in aq. ammonium bicarbonate solution, 25 mM, pH 7.5): absorbance (*green*), excitation (*blue*, $\lambda_{\text{em}} = 614 \text{ nm}$) and emission (*red*, $\lambda_{\text{exc}} = 336 \text{ nm}$).

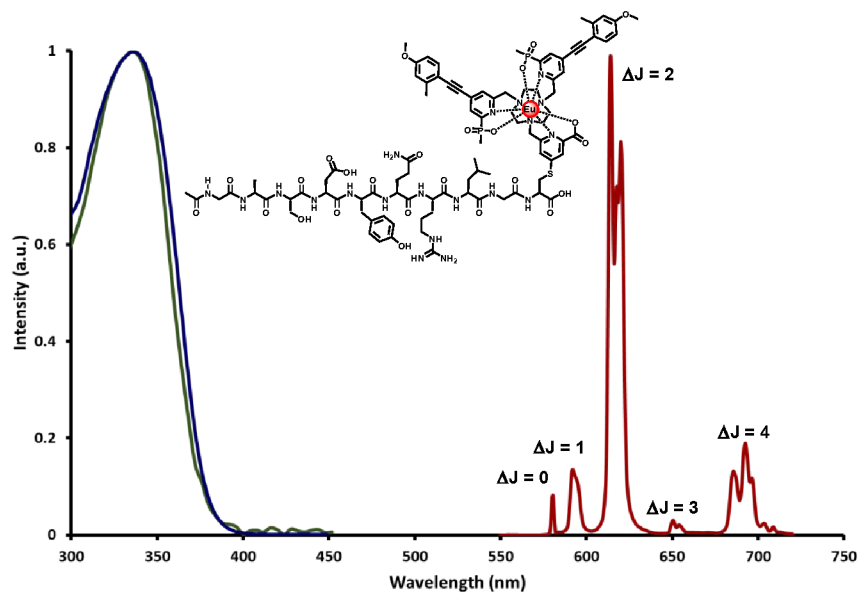


Figure 5. Photophysical spectra for $[\text{EuL}^4]$ ($25.5 \mu\text{M}$ in aq. ammonium bicarbonate solution, 25 mM , $\text{pH } 7.5$); absorbance (green), excitation (blue, $\lambda_{\text{em}} = 614 \text{ nm}$) and emission (red, $\lambda_{\text{exc}} 336 \text{ nm}$).

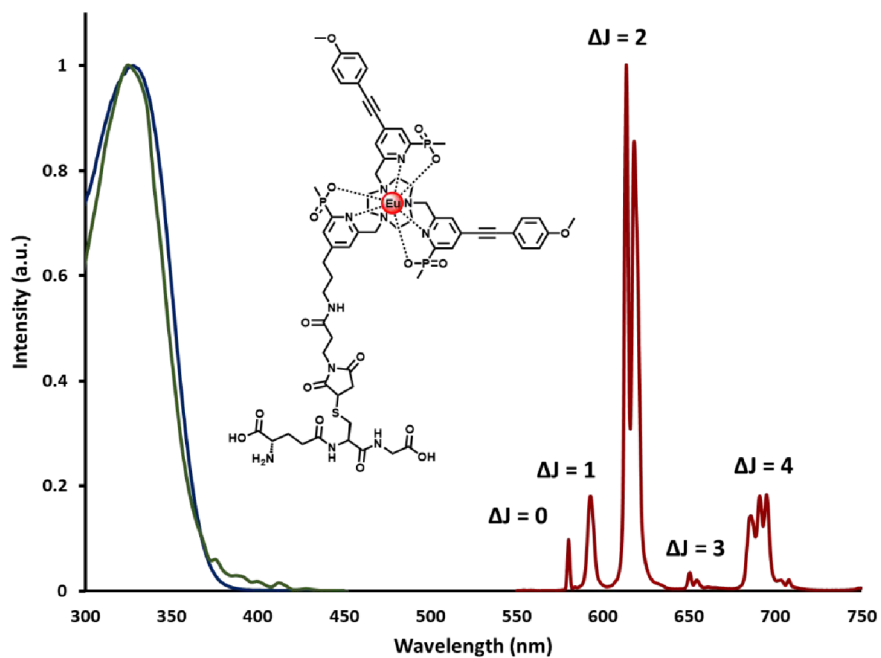


Figure 6. Photophysical spectra for $[\text{EuL}^8]$ ($18 \mu\text{M}$ in aq. ammonium bicarbonate buffer, 25 mM , $\text{pH } 7.5$); absorbance (green), excitation (blue, $\lambda_{\text{em}} = 614 \text{ nm}$) and emission (red, $\lambda_{\text{exc}} 330 \text{ nm}$).

Cell Imaging Microscopy Studies

The cell localisation behaviour of the various Eu complexes and conjugates (Chart 1) was examined as a function of time in living NIH 3T3 cells, following incubation of solutions of each complex (typically between 10 and 15 μM) in the cell growth medium. Emission spectral images and lifetimes were also recorded for the internalised complex that allowed the Eu spectral signature to be recorded; in every case the emission spectrum observed *in cellulo* was the same as that of the intact complex (e.g., Figs 4-6), and the measured emission lifetimes were within $\pm 10\%$ of those measured *in vitro*, confirming the integrity of the Eu coordination environment and the relative insensitivity of the Eu excited state to quenching.

The *p*-nitro complex, [EuL¹], gave rise to a predominant lysosomal profile, ($P_{\text{avg}} = 0.78$), as revealed by co-staining experiments with LysoTracker Green (Figure 7). Similar lysosomal localisation profiles were observed with the glutathione conjugates [EuL⁵] ($P = 0.89$), [EuL⁶] ($P = 0.78$) as well as [EuL⁸] ($P = 0.78$).

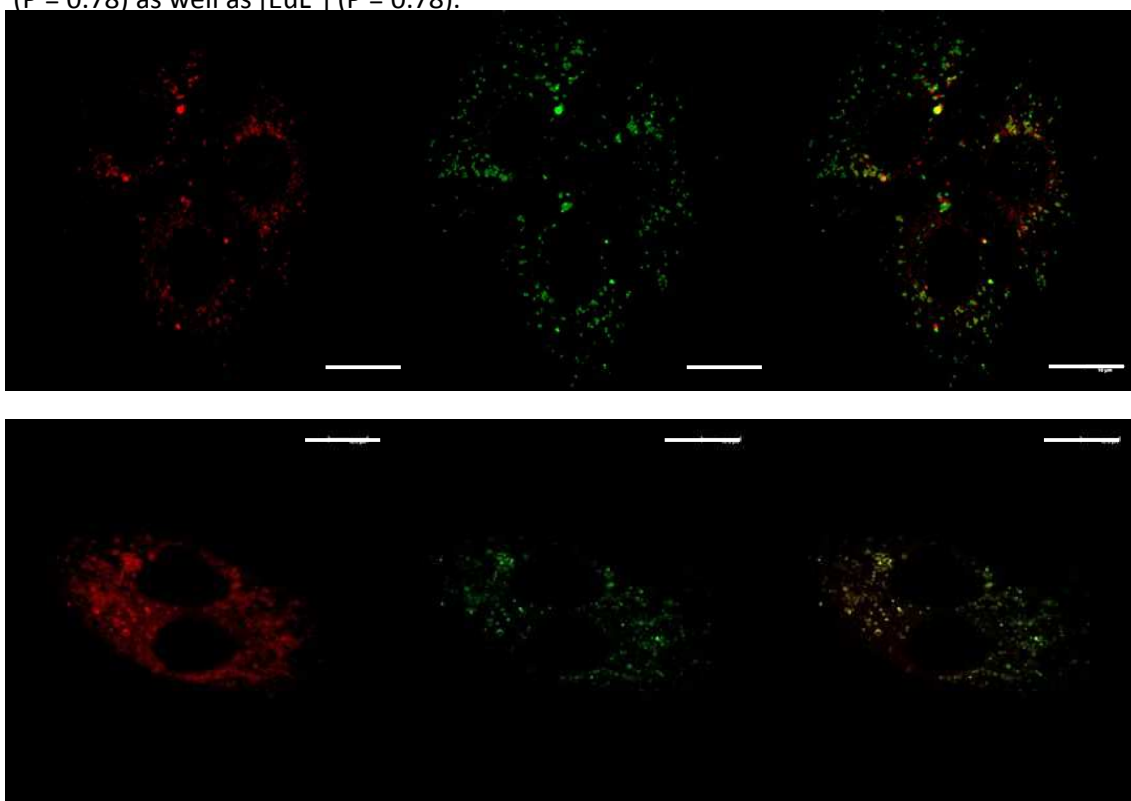


Figure 7: (*upper*: 3h, $P = 0.81$; *lower*: 23h, $P = 0.75$) Confocal microscopy images of NIH 3T3 cells following incubation with [EuL¹] (12 μM , $\lambda_{\text{exc}} = 355$ nm, observe 605 – 720 nm) (*left*); LysoTracker Green (200 nM; 5 min, $\lambda_{\text{exc}} = 488$ nm, observe 505 – 535 nm) (*centre*); (*right*): merged image showing evidence of co-localisation (scale bar 20 μm). Note the dividing cell at 23h, consistent with the behaviour of healthy living cells.

Evidence for effective targeting of the endoplasmic reticulum was observed with [EuL³] but not with [EuL⁹]. Each complex contains the ER-targeting peptide sequence 'KDEL'. In the former case, the staining of the ER was observed to increase slowly in intensity from 3 to 23h (Figure 8).

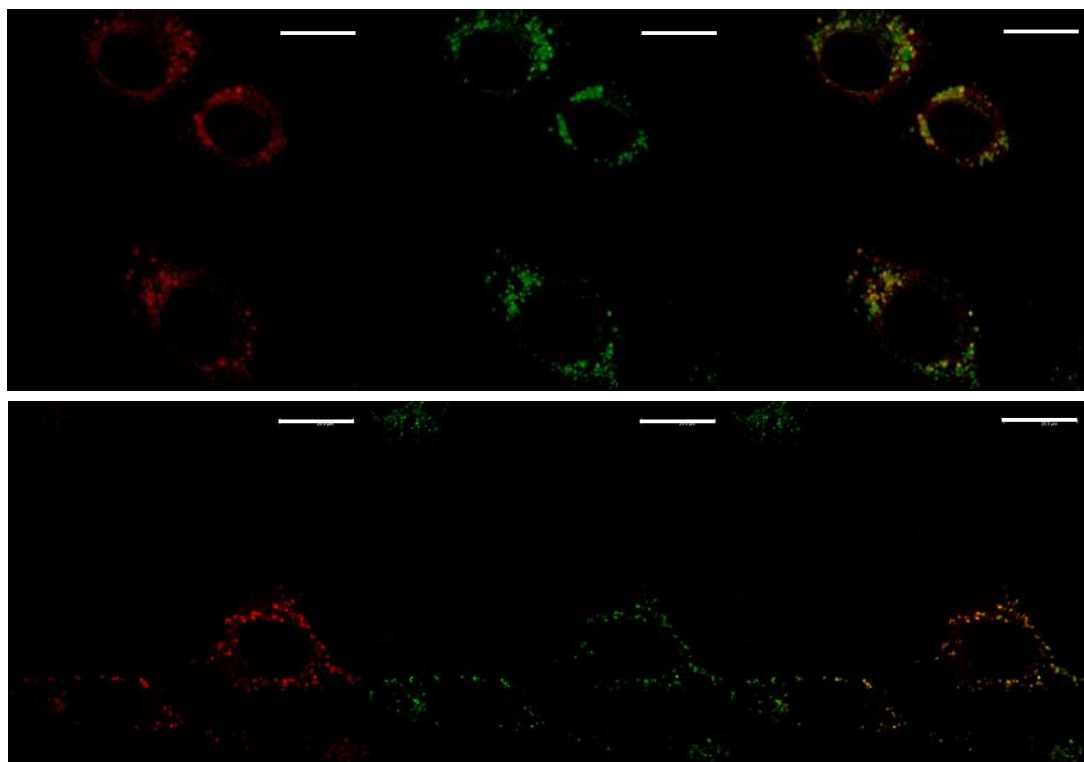


Figure 8: (upper: 3h, $P = 0.84$; lower 23h, $P = 0.89$) Confocal microscopy images of NIH 3T3 cells following incubation with **[EuL³]** (11 μM , 3 h, $\lambda_{\text{exc}} = 355$ nm, observe 605 – 720 nm) (*left*); ER-Tracker Green (200 nM; 5 min, $\lambda_{\text{exc}} = 488$ nm, observe 505 – 535 nm) (*centre*); merged image showing co-localisation in the ER (*right*), (scale bar 20 μm).

However, with the Eu complex conjugate of the peptide that has been reported to enhance localisation of the trans-Golgi network, [EuL⁴], no evidence for staining of this organelle was found, and only a simple lysosomal localisation profile was observed, ($P = 0.9$; ESI Figure S48). It is not clear whether the behaviour of [EuL⁹] reflects a lack of binding affinity of the targeting peptide, notwithstanding the success with [EuL³], or the inability of the complex to escape from a maturing endosome. Past studies have revealed that cell uptake with such europium complexes involves macropinocytosis^{12,13}, and macropinosomes are usually able to discharge their contents effectively and quite quickly within the cell.

Summary and Conclusion

A series of nine europium (III) complexes based on the 1,4,7-triazacyclononane scaffold is reported and their photophysical properties compared. The complexes show relatively high overall emission quantum yields and brightnesses in water, with values of up to 39% and 12,100 $\text{M}^{-1} \text{cm}^{-1}$ respectively. The *para*-nitro pyridyl complex, [EuL¹], allows the chemoselective linkage of a cysteine thiol group and affords stable conjugates with selected peptides, e.g. [EuL³⁻⁵], that are resistant to thiol exchange or any subsequent hydrolysis reaction. Such behaviour contrasts with that found for conjugates based on thiol attack of a

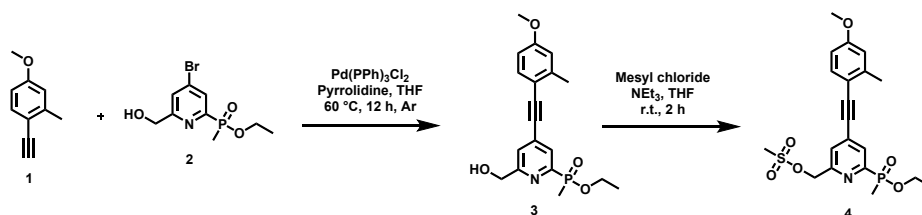
cysteine residue on a maleimide group, where further evidence is reported, e.g. with [EuL⁸] and [EuL⁹], for post-conjugation transformation. In this respect, evidence for thiol exchange is most concerning, as the europium complex is then detached from the intended targeting vector. Future conjugation strategies in creating luminescent labels for use in cell biology need to take account of such behaviour, and favour the application of the new *p*-nitrophenyl system reported herein.

Experimental

Details of reagents used and the analytical methods used (NMR, MS, optical spectroscopy and microscopy methods) are given in the supplementary information (SI).

Compounds **2**,²⁷ **7**,²⁸ **8**,²⁹ **12**³⁰ and **19**³¹ were prepared using procedures described in the literature. Compound **1** and reduced *L*-glutathione were purchased from Sigma Aldrich and CarboSynth Ltd. respectively, and the peptides with the acronyms 'ER' and 'ActGN' were supplied by Dundee Cell products. Experimental details for the preparation of [EuL²], [EuL⁵] and [EuL⁹] are given in the SI, together with selected spectra of key intermediates (Figures S1-S26), HPLC analyses of the final Eu complexes and conjugates (Figures S27-S42) and their absorption, excitation and europium emission spectra (Figures S43-S47).

Synthesis of [EuL¹]

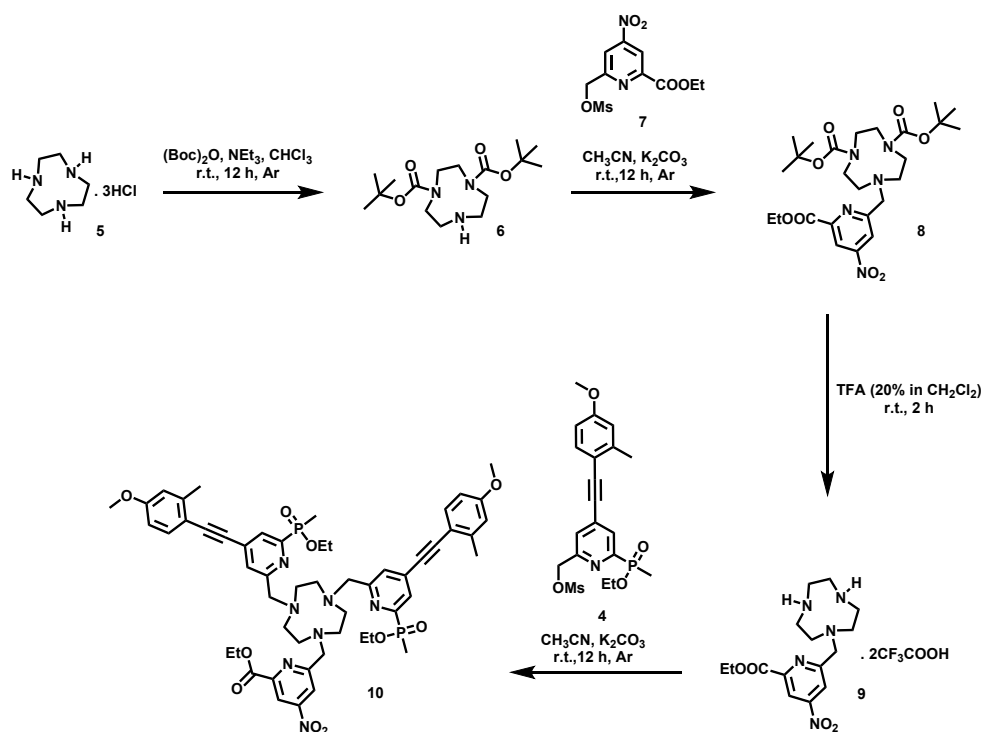


Ethyl (6-(hydroxymethyl)-4-((4-methoxy-2-methylphenyl)ethynyl)pyridin-2-yl)(methyl)phosphinate, 3. To a solution of ethyl (4-bromo-6-(hydroxymethyl)pyridin-2-yl)(methyl)phosphinate **2** (129 mg, 0.44 mmol) in anhydrous THF (2 ml) was added 1-ethynyl-4-methoxy-2-methylbenzene **1** (64.2 mg, 0.44 mmol), pyrrolidine (186 μ L, 2.20 mmol) and Pd(PPh₃)₂Cl₂ (32 mg, 0.04 mmol) under argon. The reaction was heated at 50°C under argon for 24 h. After this time, the solvent was removed under reduced pressure and the residual oil was dissolved in CH₂Cl₂ (20 ml) before addition of H₂O (20 mL). The aqueous layer was extracted with CH₂Cl₂ (3 \times 10 mL) and the combined organic layers were dried over MgSO₄, filtered, and evaporated to dryness. The crude was purified by column chromatography (Al₂O₃, CH₂Cl₂ to MeOH 2% in CH₂Cl₂) to yield compound **3** as a pale brown oil (124 mg, 78%); *R_f* (Al₂O₃, CH₂Cl₂/MeOH, 98/2) = 0.30; ¹H-NMR (298 K, 400 MHz, CDCl₃) δ _H 8.03 (dd, 1H, *J* = 6.0 Hz, *J* = 2.0 Hz), 7.50 (t, 1H, *J* = 2.0 Hz), 7.44 (d, 1H, *J* = 8.0 Hz), 6.79 (d, 1H, *J* = 2.0 Hz) 6.74 (dd, 1H, *J* = 8.0 Hz, *J* = 2.0 Hz) 4.82 (s, 2H), 4.0 (ddm, 2H, *J* = 97.0 Hz, *J* = 11.0 Hz, *J* = 7.0 Hz), 3.81 (s, 3H), 2.75 (s, 3H), 1.79 (d, 3H, *J* = 15.0 Hz), 1.28 (t, 3H, *J* = 7.0 Hz); ¹³C-NMR (298 K, 100 MHz, CDCl₃) δ _C 160.7, 152.9 (d, *J* =

155 Hz), 142.9, 134.0, 133.4 (d, $J = 11$ Hz), 128.1 (d, $J = 22$ Hz), 124.1 (d, $J = 3.0$ Hz), 115.3, 113.7, 111.6, 95.4, 89.0, 64.1, 61.4 (d, $J = 6$ Hz), 55.3, 21.0, 16.4 (d, $J = 6$ Hz), 13.4 (d, $J = 104$ Hz); $^{31}\text{P}\{^1\text{H}\}$ -NMR (298 K, 162 MHz, CDCl_3) δ_{p} +40.1; HRMS+ m/z 360.1372 $[\text{M}+\text{H}]^+$ ($\text{C}_{19}\text{H}_{23}\text{NO}_4\text{P}^+$ requires 360.1365).

(6-(Ethoxy(methyl)phosphoryl)-4-((4-methoxy-2-methylphenyl)ethynyl)pyridin-2-yl)methyl

methanesulfonate, 4. Compound **3** (123.5 mg, 0.34 mmol) was dissolved in anhydrous THF (2 mL). Methanesulfonyl chloride (33.0 μL , 0.51 mmol) and triethylamine (162 μL , 1.20 mmol) were added and the solution was stirred under argon at room temperature for 2 h. The solvent was evaporated under reduced pressure, the residue was dissolved in CH_2Cl_2 (10 mL) and brine was added (10 mL). The organic layer was separated and the aqueous layer extracted with CH_2Cl_2 (3 \times 10 mL). The combined organic layers were dried over Na_2SO_4 , filtered and concentrated to dryness to yield compound **4** as a pale yellow oil (133 mg, 88%) that was used directly in the next step without further purification; ^1H -NMR (298 K, 400 MHz, CDCl_3) δ_{H} 8.12 (dd, 1H, $J = 6.0$ Hz, $J = 2.0$ Hz), 7.64 (t, 1H, $J = 2.0$ Hz), 7.48 (d, 1H, $J = 8.0$ Hz), 6.82 (d, 1H, $J = 2.0$ Hz), 6.78 (dd, 1H, $J = 8.0$ Hz, $J = 2.0$ Hz), 5.40 (s, 2H), 4.03 (ddm, 2H, $J = 97.0$ Hz, $J = 11.0$ Hz, $J = 7.0$ Hz), 3.86 (s, 3H), 3.17 (s, 3H), 2.52 (s, 3H), 1.81 (d, 3H, $J = 15.0$ Hz), 1.31 (t, 3H, $J = 7.0$ Hz); ESI-MS m/z 438.493 (100%, $[\text{M}+\text{H}]^+$).



Di-tert-butyl 7-((6-(ethoxycarbonyl)-4-nitropyridin-2-yl)methyl)-1,4,7-triazacyclononane-1,4-

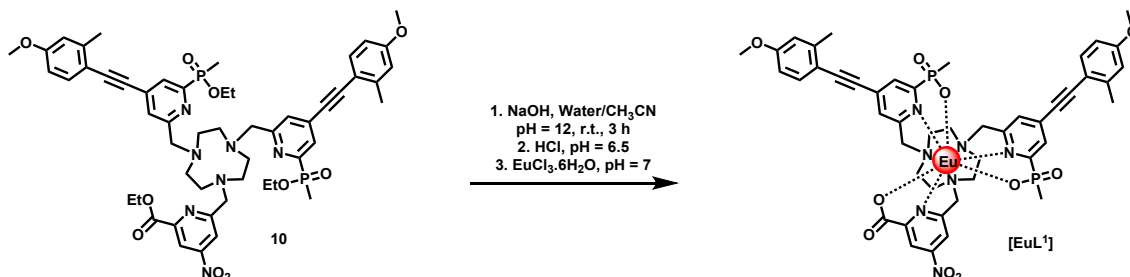
dicarboxylate, 8. Di-tert-butyl 1,4,7-triazacyclononane-1,4-dicarboxylate **6** (170 mg, 0.52 mmol) was dissolved in anhydrous CH_3CN (5 mL) under argon, and the mesylate **7** (189 mg, 0.62 mmol) and

1
2
3 K_2CO_3 (150 mg, 1.04 mmol) added. The mixture was stirred at room temperature under argon for 12
4 h. The solvent was removed under reduced pressure and the residual orange oil was dissolved in
5 CH_2Cl_2 (50 mL) before addition of H_2O (50 mL). The aqueous layer was further extracted with CH_2Cl_2
6 (3 × 25 mL) and the combined organic layers were dried over Na_2SO_4 , filtered and evaporated to
7 dryness. The residual oil was purified by reverse phase HPLC (water, 10 to 100% CH_3CN over 10 min,
8 0.1% formic acid) to yield compound **8** (205 mg, 73%, mixture of diastereoisomers) as a light yellow
9 oil; **UPLC** (water, 5 to 95% CH_3CN over 5 min, 0.1% formic acid) t_R = 2.86 min; **1H -NMR** (298 K, 400
10 MHz, $CDCl_3$) δ_H 8.56 (d, 1H, J = 2.0 Hz, isomer A), 8.54 (d, 1H, J = 2.0 Hz, isomer B), 8.44 (br s, 1H,
11 isomer A), 8.41 (br s, 1H, isomer B), 4.47 (2 × q, 2H, J = 7.0 Hz, isomers A and B respectively), 4.04 (s,
12 2H), 3.6 – 2.6 (9 br s, 12H), 1.43 (2 s, 18H, isomers B and A respectively), 1.41 (2 t, 3H, J = 7.0 Hz,
13 isomers A and B respectively); **HRMS+** m/z 538.2903 $[M+H]^+$ ($C_{25}H_{40}N_5O_8^+$ requires 538.2877).

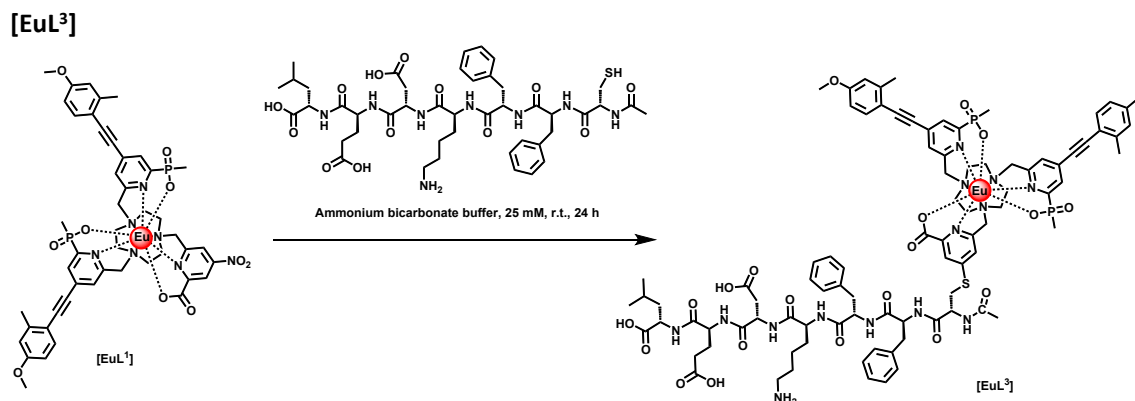
14
15
16
17
18
19
20
21 **Ethyl 6-((1,4,7-triazacyclononan-1-yl)methyl)-4-nitropicolinate, 9.** The dicarbamate **8** (70 mg, 0.13
22 mmol) was dissolved in anhydrous CH_2Cl_2 (3 mL) at room temperature. Trifluoroacetic acid (0.6 mL)
23 was added and the solution was stirred at room temperature for 2 h after which the solvent was
24 removed under reduced pressure. The residue was treated with CH_2Cl_2 (2 mL) and the solvent again
25 removed under reduced pressure; this process was repeated three times. The crude mixture was
26 purified by reverse phase HPLC (water, 10 to 100% CH_3CN over 10 min, 0.1% formic acid) to afford
27 compound **9** as its trifluoroacetate salt (70 mg, quantitative); **UPLC** (water, 5 to 95% CH_3CN over 5
28 min, 0.1% formic acid) t_R = 0.66 min; **1H -NMR** (298 K, 400 MHz, $CDCl_3$) δ_H 8.68 (d, 1H, J = 2.0 Hz), 8.18
29 (d, 1H, J = 2.0 Hz), 4.52 (q, 2H, J = 7.0 Hz), 4.37 (s, 2H), 4.3 – 3 (br. m, 12H), 1.47 (t, 3H, J = 7.0 Hz);
30 **$^{19}F\{^1H\}$ -NMR** (298 K, 376 MHz, $CDCl_3$) δ_f -75.96; **HRMS+** m/z 338.1825 $[M+H]^+$ ($C_{15}H_{24}N_5O_5^+$ requires
31 338.1828
32
33
34
35
36
37

38
39 **Ethyl 6-((4,7-bis((6-(ethoxy(methyl)phosphoryl)-4-((4-methoxy-2-methylphenyl)ethynyl)pyridin-2-
40 yl)methyl)-1,4,7-triazacyclononan-1-yl)methyl)-4-nitropicolinate, 10.** Compound **9** (6 mg, 17.8 μ mol)
41 was dissolved in anhydrous CH_3CN (1 mL) at room temperature under argon. The mesylate **4** (16.3
42 mg, 37.3 μ mol) and K_2CO_3 (11.0 mg, 70 μ mol) were added and the solution was stirred at room
43 temperature for 24 h under argon. After this time the solution was filtered and the filtrate was
44 evaporated to dryness. The subsequent residue was purified by HPLC (water, 10 to 100% CH_3CN over
45 10 min, 0.1% formic acid) to yield compound **10** (16 mg, 88%) as a pale yellow oil; **UPLC** (water, 5 to
46 95% CH_3CN over 5 min) t_R = 3.69 min; **1H -NMR** (298 K, 400 MHz, $CDCl_3$) δ_H 8.73 (d, 1H, J = 2.0 Hz), 8.60
47 (d, 1H, J = 2.0 Hz), 8.01 (dd, 2H, J = 6.0 Hz, J = 2.0 Hz), 7.65 (t, 2H, J = 2.0 Hz), 7.43 (d, 2H, J = 8.0 Hz),
48 6.79 (d, 2H, J = 2.0 Hz), 6.75 (dd, 2H, J = 8.0 Hz, J = 2.0 Hz), 4.52 (q, 2H, J = 7.0 Hz), 4.14 (s, 2H), 4.00
49 (dm, 4H, J = 90.0 Hz), 3.93 (s, 4H), 3.85 (s, 6H), 3.1 – 2.9 (br. m, 12H), 2.48 (s, 6H), 1.78 (d, 6H, J = 15.0
50 Hz), 1.46 (t, 3H, J = 7.0 Hz), 1.28 (t, 6H, J = 7.0 Hz); **^{13}C -NMR** (298 K, 100 MHz, $CDCl_3$) δ_C 164.6, 163.4,
51
52
53
54
55
56
57

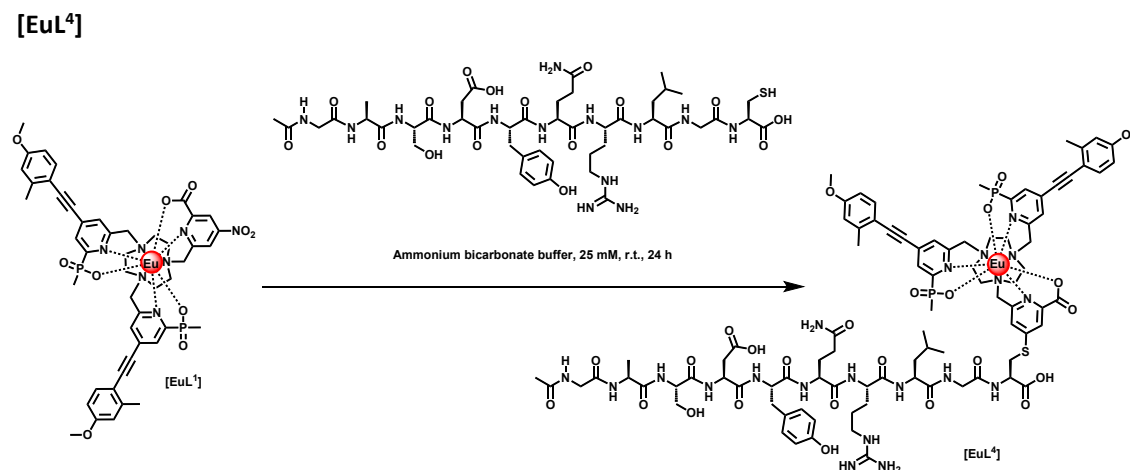
160.6, 159.5 (d, $J = 22$ Hz), 156.1, 155.4, 152.9 (d, $J = 157.0$ Hz), 142.8, 133.9, 133.4 (d, $J = 11.0$ Hz), 126.6 (d, $J = 22.0$ Hz), 125.7, 118.4, 116.1, 115.3, 113.7, 111.6, 94.6, 89.2, 62.7, 62.2, 61.0 (d, $J = 6.0$ Hz), 55.3, 54.0, 53.0, 44.7, 39.3, 21.0, 16.5 (d, $J = 6.0$ Hz), 14.3, 13.4 (d, $J = 103.0$ Hz); $^{31}\text{P}\{^1\text{H}\}$ -NMR (298 K, 162 MHz, CDCl_3) δ_{p} 40.1; **HRMS+** m/z 1020.419 $[\text{M}+\text{H}]^+$ ($\text{C}_{53}\text{H}_{64}\text{N}_7\text{O}_{10}\text{P}_2^+$ requires 1020.419).



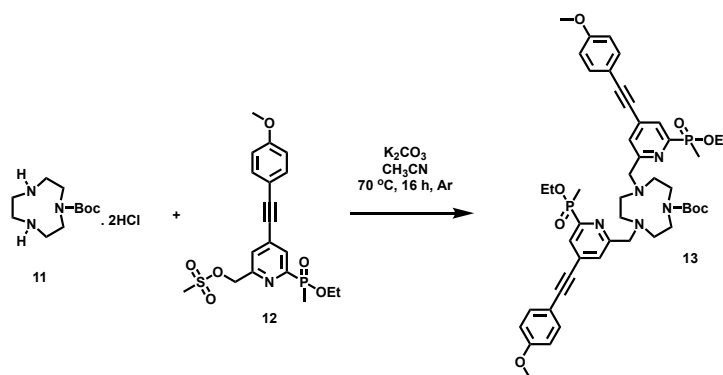
Europium complex of 6-((4,7-bis((6-(ethoxy(methyl)phosphoryl)-4-((4-methoxy-2-methylphenyl)ethynyl)pyridin-2-yl)methyl)-1,4,7-triazacyclononan-1-yl)methyl)-4-nitropicolinate, [EuL¹]. Compound **10** (15.0 mg, 14.7 μmol) was dissolved in CH_3CN (1.5 mL), and an aqueous solution of NaOH (0.5 mL, 0.1 M) was added to reach pH = 12. The solution was stirred at room temperature and ester cleavage was monitored by LC/MS until complete hydrolysis of the ligand **L¹** was observed; **HRMS+** m/z 936.3232 $[\text{M}+\text{H}]^+$ ($\text{C}_{47}\text{H}_{52}\text{N}_7\text{O}_{10}\text{P}_2^+$ requires 936.3251); $^{31}\text{P}\{^1\text{H}\}$ -NMR (298 K, 162 MHz, CDCl_3) $\delta_{\text{p}} = +26.9$ ($\delta_{\text{p}} = +40.1$ for reactant). After complete hydrolysis, the pH was adjusted to 6.5 by addition of dilute hydrochloric acid (0.1 M HCl). $\text{EuCl}_3 \cdot 6\text{H}_2\text{O}$ (11.0 mg, 29.3 μmol) was added and the solution was stirred at room temperature for 12 h. The solution was removed under reduced pressure to yield the crude Eu(III) complex as a yellow solid, displaying bright red luminescence under long-wave UV light. The complex was purified by HPLC (ammonium bicarbonate buffer, 25 mM, 10 to 100% CH_3CN in buffer over 10 min) to yield complex **[EuL¹]** (8.8 mg, 56%) as a yellow powder after freeze drying; **HRMS+** m/z 1084.222 $[\text{M}+\text{H}]^+$ ($\text{C}_{47}\text{H}_{49}\text{N}_7\text{O}_{10}\text{P}_2^{151}\text{Eu}^+$ requires 1084.221); **UPLC** (ammonium bicarbonate buffer, 25 mM, 10 to 100% CH_3CN in buffer over 10 min) $t_{\text{R}} = 5.88$ min; $\tau_{\text{H}_2\text{O}}$ (aq. ammonium bicarbonate) = 0.87 ms; $\tau_{\text{D}_2\text{O}} = 1.05$ ms; $\tau_{\text{MeOH}} = 1.15$ ms; $q = 0$; λ_{max} (H_2O) = 340 nm; $\epsilon_{340 \text{ nm}} = 42000 \text{ M}^{-1} \text{ cm}^{-1}$; $\phi_{\text{H}_2\text{O}} = 5\%$, $\phi_{\text{MeOH}} = 39\%$.



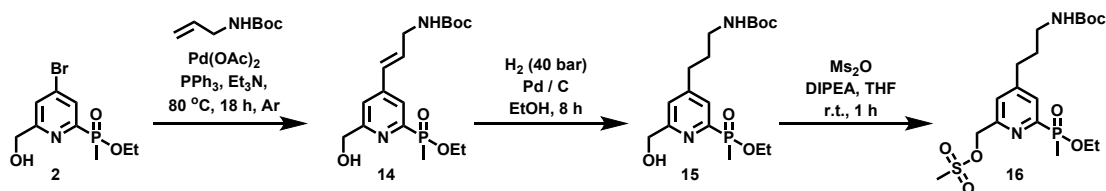
16 The complex **[EuL¹]** (0.5 mg, 0.46 μmol) was dissolved in ammonium bicarbonate buffer (2 mL, 25
17 mM in water) and the peptide 'ER' (0.48 mg, 0.51 μmol) was added. The solution was stirred at room
18 temperature for 24 h and the reaction was monitored by LC/MS. The crude solution was directly
19 purified by HPLC (ammonium bicarbonate buffer, 25 mM, 10 to 100% CH_3CN in buffer over 10 min)
20 to yield **[EuL³]** (0.37 mg, 40%); **LC/MS** (ES+ MS) m/z 1981.66 (100% $[\text{M}+\text{H}]^+$), 991.17 (69%, $\frac{[\text{M}+2\text{H}]^{2+}}{2}$);
21 **UPLC** (ammonium bicarbonate buffer, 25 mM, 10 to 100% CH_3CN in buffer over 10 min) $t_{\text{R}} = 5.69$
22 min; $\tau_{\text{H}_2\text{O}}$ (ammonium bicarbonate) = 0.93 ms; λ_{max} (H_2O) = 336 nm; $\epsilon_{336 \text{ nm}} = 41000 \text{ M}^{-1} \text{ cm}^{-1}$; $\phi_{\text{H}_2\text{O}} = 16\%$.



44 The complex **[EuL¹]** (4.06 mg, 3.74 μmol) was dissolved in ammonium bicarbonate buffer (2 mL, 25
45 mM in water) and the peptide 'ActGN' (2.00 mg, 1.80 μmol) was added. The solution was stirred at
46 room temperature for 24 h and the reaction was monitored by LC/MS. The crude solution was
47 directly purified by HPLC (ammonium bicarbonate buffer, 25 mM, 10 to 100% CH_3CN in buffer over
48 10 min) to yield the complex **[EuL⁴]** (2.3 mg, 60%); **LC/MS** (ES+ MS) m/z 2149.69 (26.5% $[\text{M}+\text{H}]^+$),
49 1075.35 (100%, $\frac{[\text{M}+2\text{H}]^{2+}}{2}$); **UPLC** (ammonium bicarbonate buffer, 25 mM, 10 to 100% CH_3CN in
50 buffer over 10 min) $t_{\text{R}} = 5.42$ min; $\tau_{\text{H}_2\text{O}} = 0.93$ ms; λ_{max} (H_2O) = 336 nm; $\epsilon_{336 \text{ nm}} = 41000 \text{ M}^{-1} \text{ cm}^{-1}$; $\phi_{\text{H}_2\text{O}} =$
51 18%.

[EuL⁶]

Compound 13. The macrocycle **11** (68 mg, 0.225 mmol), mesylate **12** (220 mg, 0.520 mmol) and K_2CO_3 (200 mg, 1.45 mmol) were combined in anhydrous CH_3CN under argon and heated at 70 °C for 16 h. After this time the crude solution was separated from the inorganic salts by filtration and purified directly by reverse phase HPLC (water, 10 to 100% CH_3CN over 10 min) to yield compound **13** as a pale yellow oil (126 mg, 63%); UPLC (water, 5 to 95% CH_3CN over 5 min) $t_R = 2.46$ min; **¹H-NMR** (298 K, 600 MHz, $CDCl_3$) δ_H 7.99 (app. t, 2H, $J = 5.6$ Hz), 7.67 (s, 1H), 7.58 (s, 1H), 7.47 (d, 4H, $J = 8.5$ Hz), 6.89 (d, 4H, $J = 7.6$ Hz), 4.14 – 4.05 (m, 2H), 3.95 (d, 4H), 3.90 – 3.81 (m, 2H), 3.83 (s, 6H), 3.43 – 3.32 (m, 4H), 3.15 – 3.04 (m, 4H), 2.76 – 2.63 (m, 4H), 1.76 (2 × d, 6H, $J = 15$ Hz), 1.48 (s, 9H), 1.25 (2 × t, 6H, $J = 7.0$ Hz); **³¹P-NMR** (298 K, 162 MHz, $CDCl_3$) $\delta_P +40.1$ (2 × s); **HRMS+** m/z 884.3937 [$M+H$]⁺ ($C_{47}H_{59}N_5O_8P_2$ requires 884.3940).



tert-Butyl-(E)-(3-(2-(ethoxy(methyl)phosphoryl)-6-(hydroxymethyl)pyridin-4-yl)allyl)carbamate, 14. Compound **2** (74 mg, 0.25 mmol), *tert*-butyl *N*-allylcarbamate (155 mg, 0.99 mmol), palladium(II) acetate (11 mg, 0.05 mmol) and triphenylphosphine (20 mg, 0.08 mmol) were combined in toluene (2 mL) under an argon atmosphere. The reaction mixture was degassed by bubbling through with argon for 15 min. Following this, triethylamine (0.3 mL, 2.2 mmol) was added and the mixture was heated to 80 °C under argon for 18 h. After cooling, the solvent was removed under reduced pressure and the resulting residue dissolved in CH_2Cl_2 (30 mL), washed with water (4 × 30 mL) and dried over $MgSO_4$. Removal of the solvent under reduced pressure gave the crude product **14**. Further purification by reverse phase HPLC (water, 10 to 100% CH_3CN over 10 min) yielded compound **14** as an *E/Z* isomer mixture (93 mg, 63%); **¹H-NMR** (298 K, 400 MHz, $CDCl_3$) δ_H 8.03 – 7.91 (2 × d, 1H), 7.45 – 7.28 (2 × s, 1H), 6.61 – 6.44 (m, 2H), 4.83 – 4.77 (2 × s, 2H), 4.14 – 4.03 & 3.89 –

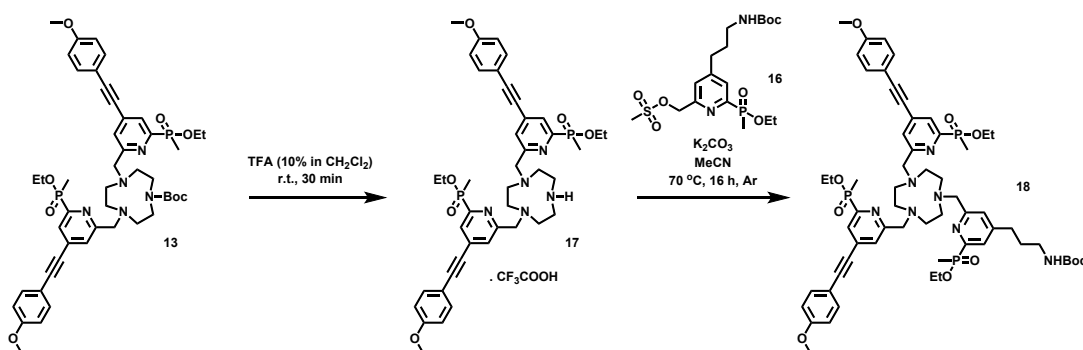
3.77 (m, 2H), 3.97 – 3.93 (m, 2H), 1.80 – 1.74 (2 × d, 3H), 1.48 – 1.40 (2 × t, 3H); $^{31}\text{P}\{^1\text{H}\}$ -NMR (298 K, 162 MHz, CDCl_3) δ_{P} +40.5, +40.4; HRMS+ m/z 371.1746 $[\text{M}+\text{H}]^+$ ($\text{C}_{17}\text{H}_{28}\text{N}_2\text{O}_5\text{P}^+$) requires 371.1736.

tert-Butyl (3-(2-(ethoxy(methyl)phosphoryl)-6-(hydroxymethyl)pyridin-4-yl)propyl)carbamate, 15.

The *E/Z* isomer mixture of compound **14** (210 mg, 0.57 mmol) was dissolved in ethanol (60 mL) to which palladium upon carbon (Pd content 10%, 25 mg) was added. The vessel was then loaded onto a Parr hydrogenator (pressure 40 bar H_2) and the reaction mixture was agitated for 8 h. After this time, the catalyst was removed by filtration and the solvent removed under reduced pressure. Compound **15** was dried under high vacuum and isolated as a pale yellow oil (210 mg); ^1H -NMR (298 K, 600 MHz, CDCl_3) δ_{H} 7.82 (d, 1H, $J = 6$ Hz), 7.24 (s, 1H), 4.78 (s, 2H), 4.66 (br s, 1H), 4.12 – 3.79 (m, 2H), 3.18 – 3.11 (m, 2H), 2.73 – 2.68 (m, 2H), 1.87 – 1.81 (m, 2H), 1.76 (d, 3H, $J = 15$ Hz), 1.43 (s, 9H), 1.26 (t, 3H, $J = 7$ Hz); ^{13}C -NMR (298 K, 151 MHz, CDCl_3) δ_{C} 160.5 (d, $J = 19$), 156.1, 153.0 (d, $J = 156$), 152.2 (d, $J = 10$), 127.0 (d, $J = 21$), 123.0, 79.5, 64.1, 61.2 (d, $J = 6$), 40.0, 32.6, 30.8, 28.5, 16.6 (d, $J = 6$), 13.7 (d, $J = 104$); $^{31}\text{P}\{^1\text{H}\}$ -NMR (298 K, 243 MHz, CDCl_3) δ_{P} +39.9; HRMS+ m/z 373.1880 $[\text{M}+\text{H}]^+$ ($\text{C}_{17}\text{H}_{30}\text{N}_2\text{O}_5\text{P}^+$ requires 373.1892); $R_f = 0.40$ (5% CH_3OH in CH_2Cl_2).

(4-(3-((tert-Butoxycarbonyl)amino)propyl)-6-(ethoxy(methyl)phosphoryl)pyridin-2-yl)methyl methanesulfonate, 16.

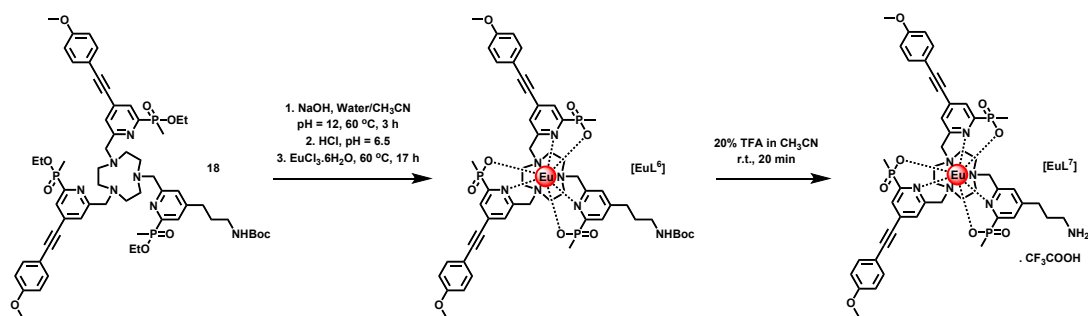
Compound **15** (25 mg, 0.067 mmol), methanesulfonic anhydride (20 mg, 0.115 mmol) and DIPEA (0.03 mL, 0.172 mmol) were combined in anhydrous THF (0.5 mL) under argon. The reaction mixture was stirred at room temperature for 1 h with monitoring by TLC. Following complete conversion, the solvent was removed under reduced pressure and the resulting crude residue dissolved in CH_2Cl_2 (40 mL), washed with water (3 × 40 mL) and the organic layer dried over K_2CO_3 . Removal of the solvent under reduced pressure afforded the mesylate **16** as a colourless oil (30 mg, quant.); ^1H -NMR (298 K, 400 MHz, CDCl_3) δ_{H} 7.86 (d, 1H, $J = 6$ Hz), 7.41 (s, 1H), 5.33 (s, 2H), 4.66 (br s, 1H), 4.15 – 3.77 (m, 2H), 3.19 – 3.09 (m, 5H), 2.76 – 2.67 (m, 2H), 1.89 – 1.79 (m, 2H), 1.74 (d, 3H, $J = 15$ Hz), 1.42 (s, 9H), 1.25 (t, 3H, $J = 7.1$ Hz); HRMS+ m/z 451.1666 $[\text{M}+\text{H}]^+$ ($\text{C}_{18}\text{H}_{32}\text{N}_2\text{O}_7\text{PS}^+$ requires 451.1668); $R_f = 0.50$ (5% CH_3OH in CH_2Cl_2).



Compound 17. Trifluoroacetic acid (0.8 mL) was added to a solution of compound **13** (73 mg, 0.082 mmol) in CH₂Cl₂ (3.2 mL). The solution was stirred at room temperature for 40 min before removal of the solvent under reduced pressure. To the subsequent residue was added CH₂Cl₂ (20 mL) and the solvent was removed under reduced pressure once again; this process was repeated five times. The residue was dried under high vacuum for several hours to yield the named compound **17** as the trifluoroacetate salt (74 mg, quant.); ¹H-NMR (298 K, 700 MHz, CDCl₃) δ_H 7.82 (d, 2H, *J* = 6 Hz), 7.49 – 7.45 (m, 6H), 6.89 (d, 4H, *J* = 9 Hz), 4.32 (s, 4H), 4.15 – 4.08 & 3.99 – 3.91 (m, 4H), 3.82 (s, 6H), 3.60 – 3.44 (m, 8H), 3.36 – 3.23 (m, 4H), 1.74 (d, 6H, *J* = 15 Hz), 1.30 (dt, 6H, *J* = 7.1 Hz, *J* = 2 Hz); ¹³C-NMR (298 K, 176 MHz, CDCl₃) δ_C 161.1, 156.7 (d, *J* = 17 Hz), 153.3 (d, *J* = 160 Hz), 134.4 (d, *J* = 12 Hz), 133.9, 128.0 (d, *J* = 23 Hz), 127.5, 114.4, 113.3, 98.0, 84.6, 62.4 (d, *J* = 6 Hz), 59.8, 55.5, 51.6, 49.7, 44.5, 16.4 (d, *J* = 6 Hz), 13.7 (d, *J* = 102 Hz); ³¹P{¹H}-NMR (298 K, 162 MHz, CDCl₃) δ_p +40.9, +40.8; HRMS+ *m/z* 784.3415 [M+H]⁺ (C₄₂H₅₂N₅O₆P₂⁺ requires 784.3393).

Compound 18. The macrocycle **17** (74 mg, 0.082 mmol), mesylate **16** (90 mg, 0.20 mmol) and K₂CO₃ (90 mg, 0.65 mmol) were combined in anhydrous CH₃CN (2 mL) under argon and heated at 70 °C for 16 h. After this time the crude solution was separated from the inorganic salts by filtration and purified directly by reverse phase HPLC (water with 0.1% formic acid, 10 to 100% CH₃CN with 0.1% formic acid over 10 min) to yield a pale orange oil (38 mg, 40%); ¹H-NMR (298 K, 400 MHz, CH₃OD) δ_H 8.48 (s, 1H), 7.93 (d, 2H, *J* = 5.7 Hz), 7.84 (d, 1H, *J* = 6 Hz), 7.68 (s, 2H), 7.50 (d, 4H, *J* = 8.6 Hz), 6.98 (d, 4H, *J* = 8.6 Hz), 4.36 (br s, 2H), 4.27 – 4.19 (m, 6H), 4.17 – 3.93 (m, 6H), 3.84 (s, 6H), 3.29 – 3.08 (m, 12H), 3.05 (t, 2H, *J* = 6.7 Hz), 2.76 (t, 2H, *J* = 7.5 Hz), 1.88 – 1.80 (m, 9H), 1.42 (s, 9H), 1.31 – 1.26 (m, 9H); ¹³C-NMR (298 K, 176 MHz, CH₃OD) δ_C 169.3, 162.6, 159.3 (2 × d, *J* = 19 Hz), 158.5 (2 × d, *J* = 10 Hz), 155.4 (2 × d, *J* = 160 Hz), 134.8, 128.7 (d, *J* = 5 Hz), 128.6 (d, *J* = 23 Hz), 128.3 (d, *J* = 23 Hz), 115.5, 114.5, 98.0, 85.8, 79.9, 63.0 (d, *J* = 6 Hz), 62.9 (d, *J* = 6 Hz), 60.3, 59.8, 56.0, 51.4, 51.0, 50.3, 40.5, 33.2, 31.5, 28.8, 16.9 (2 × d, *J* = 6 Hz), 13.4 (d, *J* = 102 Hz), 13.3 (d, *J* = 102 Hz); ³¹P{¹H}-NMR (298 K, 162 MHz, CH₃OD) δ_p +41.8, +41.2; HRMS+ *m/z* 1138.512 [M+H]⁺ (C₅₉H₇₈N₇O₁₀P₃⁺ requires 1138.510).

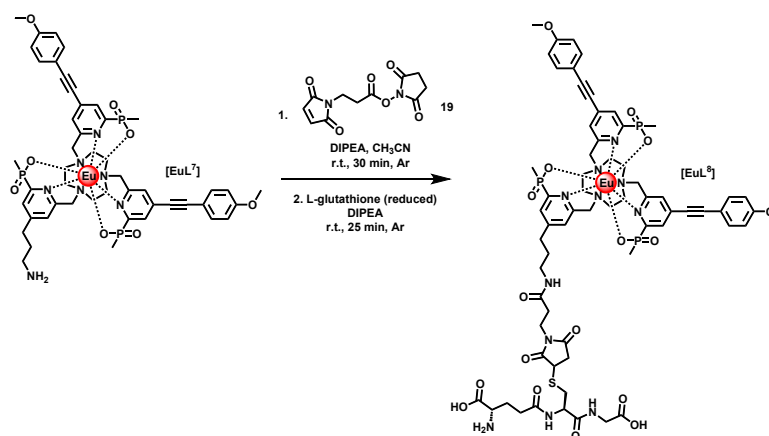
Synthesis of [EuL⁷]



[EuL⁶]. The ligand precursor **18** (10 mg, 0.009 mmol) was dissolved in a solution of CH₃OH/water (1.5:1, 2.5 mL total) and the pH was adjusted to 12 using a NaOH solution (4 M). The solution was heated at 60 °C for 3 h with monitoring by LC/MS. After complete hydrolysis of the ester groups, the pH of the solution was readjusted to 6.5 using a HCl solution (2 M) and EuCl₃·6H₂O (4 mg, 0.011 mmol) was added. The mixture was heated at 60 °C once again for 17 h. After this time, the mixture was filtered and the solution purified by reverse phase HPLC (water, 10 to 100% CH₃OH over 10 min) to yield the complex **[EuL⁶]** as a white solid (5 mg, 46%); **HRMS+** *m/z* 1202.31 [M+H]⁺ (C₅₃H₆₄N₇O₁₀P₃¹⁵¹Eu⁺ requires 1202.31); UPLC (ammonium bicarbonate buffer, 25 mM, 10 to 100% CH₃CN in buffer over 10 min) *t_R* = 2.95 min; *τ*_{H₂O} = 1.11 ms; *τ*_{MeOH} = 1.27 ms, *λ*_{max} = 328 nm; *ε*_{328 nm} = 31000 M⁻¹ cm⁻¹; *φ*_{H₂O} = 33%.

[EuL⁷]. Trifluoroacetic acid (0.8 mL) was added to a solution of **[EuL⁶]** (7.2 mg, 6.0 μmol) in CH₃CN (3.2 mL). The solution was stirred at room temperature for 20 min before removal of the solvent under reduced pressure. To the subsequent residue was added CH₃CN (20 mL) and the solvent was removed under reduced pressure once again; this process was repeated five times. The residue was dried under high vacuum for several hours to yield the complex **[EuL⁷]** as the trifluoroacetic salt (7.8 mg, quant.); **HRMS+** *m/z* 1104.260 [M+H]⁺ (C₄₈H₅₆N₇O₈P₃¹⁵¹Eu⁺ requires 1104.262); UPLC (ammonium bicarbonate buffer, 25 mM, 10 to 100% CH₃CN in buffer over 10 min) *t_R* = 2.75 min.

[EuL⁸]



[EuL⁸]. To a solution of the complex **[EuL⁷]** (7.8 mg, 6.0 μmol) in anhydrous CH₃CN under argon was added the active ester **19** (1.4 mg, 5.3 μmol) and DIPEA (0.05 mL, excess). The solution was stirred at room temperature under argon for 30 min at which point the formation of the maleimide derivative **[EuL⁷-maleimide]** was confirmed by mass spectrometry (**HRMS+** *m/z* 1255.29 [M+H]⁺ (C₅₅H₆₁N₈O₁₁P₃¹⁵¹Eu⁺ requires 1255.29)). Reduced L-glutathione (1.6 mg, 5.3 μmol) was added to the solution and the reaction was stirred at room temperature for a further 30 min. The reaction mixture

1
2
3 was directly subjected to reverse phase HPLC (ammonium bicarbonate buffer, 25 mM, 10 to 100%
4 CH₃CN in buffer over 10 min) to yield the complex **[EuL⁸]** as a white solid (1 mg, 12% over two steps);
5 **HRMS+** *m/z* 1562.38 [M+H]⁺ (C₆₅H₇₈N₁₁O₁₇P₃S¹⁵¹Eu⁺ requires 1562.37); UPLC (ammonium bicarbonate
6 buffer, 25 mM, 10 to 100% CH₃CN in buffer over 10 min) *t_R* = 2.75 min; *τ*_{H₂O} = 1.09 ms; *λ*_{max} = 328 nm;
7
8

9 $\epsilon_{328} \quad \text{nm} \quad = \quad 31000 \quad \text{M}^{-1} \quad \text{cm}^{-1}; \quad \phi_{\text{H}_2\text{O}} \quad = \quad 28\%.$
10
11
12
13
14
15
16
17
18
19
20
21
22
23
24
25
26
27
28
29
30
31
32
33
34
35
36
37
38
39
40
41
42
43
44
45
46
47
48
49
50
51
52
53
54
55
56
57
58
59
60

AUTHOR INFORMATION

Corresponding Author

*E-mail: david.parker@dur.ac.uk

Notes

The authors declare no conflicting interests.

ACKNOWLEDGEMENTS

We thank the Royal Society (RP), the EPSRC (MS, grant /EP 025013/1) and Cisbio Bioassays (JDF) for support. Supporting information is available (45 pages), detailing ligand, complex and conjugate syntheses and multinuclear NMR spectra, HPLC analyses, photophysical data, confocal microscopy images and instrumentation and general experimental methods.

REFERENCES

1. Parker, D. (2016) Rare Earth Coordination Chemistry in Action, in *Handbook on the Physics and Chemistry of Rare Earths, Volume 50*, pp 269–299.
2. Matthieu, E., Sipos, A., Demayere, E., Phipps, D., Sakaveli, D., Borbas, K. E. (2018) Lanthanide-based tools for the investigation of cellular environments. *Chem. Commun.* **54**, 10021-10035.
3. Montgomery, C. P., Murray, B. S., New, E. J., Pal, R., Parker, D. (2009) Cell penetrating metal complexes as optical probes: a mechanistic approach to targeted responsive systems based on lanthanide luminescence *Acc. Chem. Res.* **42**, 925-937.
4. Rajendran, M., Miller, L.W. (2015) Evaluating the performance of time-gated live-cell microscopy with lanthanide probes. *Biophys. J.* **109**, 240-248.
5. Ning, Y., Tang, J., Liu, Y. W., Jing, J., Sun, Y. and Zhang, J. L. (2018) Highly luminescent, biocompatible ytterbium(III) complexes as near-infrared fluorophores for living cell imaging. *Chem. Sci.* **9**, 3742–3753.
6. Jiang, L., Lan, R., Li, H., Lear, S., Zong, J., Wong, W.-Y., S., Law, G-L., Wong, W-T., Cobb, S. L., Wong, K.-L. *et al* (2017) EBNA1-targeted probe for the imaging and growth inhibition of tumours associated with the Epstein–Barr virus. *Nat. Biomed. Eng.* **1**, 0042-0049.
7. Heffern, M. C., Matosziuk, L. M. and Meade, T. J. (2014) Lanthanide probes for bioresponsive imaging. *Chem. Rev.* **114**, 4496–4539.
8. Oueslati, N., Hounsou, C., Belhocine, A., Rodriguez, T., Dupuis, E., Zwier, J. M., Trinquet, E., Pin, J. P., Durroux, T. G. (2015) G-protein-coupled receptor screening assays: methods and protocols. *Methods in Molecular Biology* **1272**, 23-36.
9. Murray, B. S., New, E. J., Pal, R. and Parker, D. (2008) Critical evaluation of five emissive europium(III) complexes as optical probes: correlation of cytotoxicity, anion and protein affinity with complex structure, stability and intracellular localisation profile. *Org. Biomol. Chem.* **6**, 2085-2094.
10. Kielar, F., New, E. J., Law, G-L. and Parker, D. (2008) The nature of the sensitiser substituent determines quenching sensitivity and protein affinity and influences the

- 1
2
3 design of emissive lanthanide complexes as optical probes for intracellular use. *Org.*
4 *Biomol. Chem.* **6**, 2256-2258.
- 5 11. New, E. J., Smith, D. G., Walton, J. W. and Parker, D. (2010) Development of responsive
6 lanthanide probes for cellular applications. *Curr. Opin. Chem. Biol.* **14**, 238-246.
- 7 12. New, E. J., Congreve, A., Pal, R. and Parker D. (2010) Definition of the uptake mechanism
8 and sub-cellular localisation profile of emissive lanthanide complexes as cellular optical
9 probes. *Chem. Sci.* **1**, 111-118.
- 10 13. Frawley, A. T., Linford, H. V., Starck, M., Pal, R., and Parker, D. (2018) Enantioselective
11 cellular localisation of europium(III) coordination complexes. *Chem. Sci.* **9**, 1042-1048.
- 12 14. Zou, Z., Rajendran, M., Magda, D., Miller, L. W. (2015) Cytoplasmic delivery and selective,
13 multi-component labeling with oligoarginine-linked protein tags. *Bioconjugate Chem.* **26**,
14 460-465.
- 15 15. Cieslikiewicz, M., Eliseeva, S. V., Aucagne, V., Delmas, A. F., Gilaizeau, I., Petoud, S. (2019)
16 Near-infrared emitting lanthanide(III) complexes as prototypes of optical imaging agents
17 with peptide targeting ability: a methodological approach. *RSC Advances* **9**, 1747-1751.
- 18 16. Kielar, F., Congreve, A., Law, G-L., New, E. J., Parker, D., Wong, K-L., Castrenos, P., de
19 Mendoza, J. (2008) Two photon microscopy study of the intracellular
20 compartmentalisation of selected emissive terbium complexes and their oligoarginine
21 and oligoguanidinium conjugates. *Chem. Commun.* 2435-24537.
- 22 17. Trychta, K. A., Back, S., Henderson, M. J., Harvey, B. K. (2018) KDEL receptors are
23 differentially regulated to maintain the er proteome under calcium deficiency. *Cell*
24 *Reports* **25**, 1829-1840.
- 25 18. Xu, A., Tang, Y., Lin, W. (2018) Endoplasmic reticulum-targeted two-photon turn-on
26 fluorescent probe for nitroreductase in tumor cells and tissues. *Spectrochim. Acta A* **770**-
27 776.
- 28 19. Pap, E. H. W., Dansen, T. B., van Summeren, R. and Wirtz, K. W. A. (2001) Peptide based
29 targeting of fluorophores to organelles in living cells. *Experimental Cell Res.* **265**, 288-293.
- 30 20. Nilsson, T. and Warren, G. (1994) Retention and retrieval in the endoplasmic reticulum
31 and the Golgi apparatus. *Curr. Opin. Chem. Biol.* **6**, 517-521.
- 32 21. Butler, S. J., Lamarque, L., Pal, R., and Parker D. (2014) EuroTracker dyes: highly emissive
33 europium complexes as alternative organelle stains for live cell imaging. *Chem. Sci.* **5**,
34 1750-1756.
- 35 22. Starck, M., Pal, R. and Parker D. (2016) Structural control of cell permeability with highly
36 emissive europium(III) complexes permits different microscopy applications. *Chem. Eur.*
37 *J.* **22**, 570-580.
- 38 23. Butler, S. J., Gempf, K. L., Funk, A. M., Parker D. (2013) Direct and selective tagging of Cys
39 residues in peptides and proteins with coordinated 4-nitropyridyl lanthanide complexes.
40 *Chem. Commun.* **49**, 9104-9106.
- 41 24. Shah, A., Roux, A., Starck, M., Mosely, J. A., Stevens, M., Norman, D. G., Hunter, R. I.,
42 Parker, D., Lovett, J. E. *et al* (2019) A new gadolinium spin label with both a narrow
43 central transition and short tether for use in double electron electron resonance distance
44 measurements. *Inorg. Chem.* **58**, 3015-3025.
- 45 25. Fontaine, S. D., Reid, R., Robinson, L., Ashley, G. W., Santi, D. V. (2015) Long-term
46 stabilization of maleimide-thiol conjugates. *Bioconjugate Chem.* **26**, 145-152.
- 47
48
49
50
51
52
53
54
55
56
57
58
59
60

- 1
2
3 26. Beeby, A., Clarkson, I. M., Dickins, R. S., Faulkner, S., Parker, D., Royle, L., de Sousa, A. S.,
4 Williams, J. A. G., Woods, M. (1999) Non-radiative deactivation of the excited states of
5 europium, terbium and ytterbium complexes by energy matched OH, NH and CH
6 oscillators: an improved luminescence method for establishing solution hydration states.
7 *J. Chem. Soc., Perkin Trans. 2*, 493-503.
- 8
9 27. Evans, N. H., Carr, R., Delbianco, M., Pal, R., Yufit, D. S. and Parker, D. (2013) Complete
10 stereocontrol in the synthesis of macrocyclic lanthanide complexes: direct formation of
11 enantiopure systems for circularly polarised luminescence applications. *Dalton Trans.*,
12 *42*, 15610-15616.
- 13
14 28. Walton, J. W., Carr, R., Evans, N. H., Funk, A. M., Kenwright, A. M., Parker, D., Yufit, D. S.,
15 Botta, M., De Pinto S. and Wong, K-L. (2012) Isostructural series of chiral nine-coordinate
16 lanthanide complexes based on triazacyclononane. *Inorg. Chem.* *51*, 8042-8056.
- 17
18 29. Mion, G., Gianferrara, T., Bergamo, A., Gasser, G., Pierroz, V., Rubbiani, R., Vilar, R.,
19 Leczkowska, A., and Alessio, E. (2015) Phototoxic activity and DNA interactions of water-
20 soluble porphyrins and their rhenium(I) conjugates. *ChemMedChem*, *10*, 1901-1914.
- 21
22 30. Walton, J. W., Bourdolle, A., Butler, S. J., Soulie, M., Delbianco, M., McMahon, B. K., Pal,
23 R., Lamarque, L., Maury, O., Parker, D. et al (2013) Very bright europium complexes that
24 stain cellular mitochondria. *Chem. Commun.*, *49*, 1600-1602.
- 25
26 31. Nielsen, O., and Buchardt, O. (1991) Facile synthesis of reagents containing a terminal
27 maleimido ligand linked to an active ester. *Synthesis*, 819-821.
- 28
29
30
31
32
33
34
35
36
37
38
39
40
41
42
43
44
45
46
47
48
49
50
51
52
53
54
55
56
57
58
59
60

FOR TABLE OF CONTENTS ONLY

The Eu complex peptide conjugate with a short tether to the ligand targets the endoplasmic reticulum effectively

